REPORT DOCUMENTATION PAGE

Public reporting burden for this collection of information is estimated to average 1 hour per response, including the time for reviewing instructions, searching existing data sources, gathering and maintaining the data needed, and completing and reviewing this collection of information. Send comments regarding this burden estimate or any other aspect of this collection of information, including suggestions for reducing this burden to Washington Headquarters Services, Directorate for Information Operations and Reports, 1215 Jefferson Davis Highway, Suite 1204, Arlington, VA 22202-4302, and to the Office of Management and Budget, Paperwork Reduction Project (0704-0188), Washington, DC 20503

1. AGENCY USE ONLY (Leave blank)	2. REPORT DATE May 2000	3. REPORT TYPE AND DATES COVERED Annual (20 Apr 99 - 19 Apr 00)	
4. TITLE AND SUBTITLE Development of Digital Steroscopic Imaging Technique in Mammography		**5. FUNDING NUMBERS** DAMD17-98-1-8210	
6. AUTHOR(S) Heang Ping Chan, Ph.D.			
7. PERFORMING ORGANIZATION NAME(S) AND ADDRESS(ES) University of Michigan Ann Arbor, Michigan 48109-1274 E-MAIL: chanhp@umich.edu		**8. PERFORMING ORGANIZATION REPORT NUMBER**	
9. SPONSORING / MONITORING AGENCY NAME(S) AND ADDRESS(ES) U.S. Army Medical Research and Materiel Command Fort Detrick, Maryland 21702-5012		**10. SPONSORING / MONITORING AGENCY REPORT NUMBER**	

11. SUPPLEMENTARY NOTES

12a. DISTRIBUTION / AVAILABILITY STATEMENT Approved for public release; distribution unlimited	12b. DISTRIBUTION CODE

13. ABSTRACT *(Maximum 200 Words)*

The goal of this research is to develop stereoscopic techniques for mammographic imaging and to investigate the feasibility of using stereomammography to improve the sensitivity of mammography for breast cancer detection, especially in dense breasts.

During this year, we have assembled a high-resolution stereoscopic viewing station and developed software for displaying and manipulating stereoscopic images. This viewing station facilitates our studies of various image acquisition and display techniques for stereoscopic imaging. Various 3D virtual cursor shapes were studied and two were chosen for an observer study to evaluate their effects on depth measurement. An observer study was also performed to study the effects of imaging techniques (x-ray dose and stereo-angles) on depth perception. The results of these experiments indicate that the 3D virtual cursors can provide absolute measurement of lesion (in particular, fibril) size and depth in the breast. The accuracy of the measurements depends on matching of the object shape and cursor shape. It was also found that depth perception depends on the quality of the stereo-images. This information is important for designing optimal imaging techniques to generate stereomammograms and for designing proper 3D virtual cursors to quantify lesion size and depth in stereomammograms. The improvement in perception of the details of mammographic features and the additional size and depth information are expected to improve diagnostic accuracy of mammographic abnormalities.

14. SUBJECT TERMS Breast Cancer Mammography, stereoscopic imaging, depth perception, breast cancer detection			15. NUMBER OF PAGES 59
			16. PRICE CODE

17. SECURITY CLASSIFICATION OF REPORT Unclassified	18. SECURITY CLASSIFICATION OF THIS PAGE Unclassified	19. SECURITY CLASSIFICATION OF ABSTRACT Unclassified	20. LIMITATION OF ABSTRACT Unlimited

NSN 7540-01-280-5500

Standard Form 298 (Rev. 2-89)
Prescribed by ANSI Std. Z39-18
298-102

20010228 008

AD_____

Award Number: DAMD17-98-1-8210

TITLE: Development of Digital Stereoscopic Imaging Technique in Mammography

PRINCIPAL INVESTIGATOR: Heang Ping Chan, Ph.D.

CONTRACTING ORGANIZATION: University of Michigan
Ann Arbor, Michigan 48109-1274

REPORT DATE: May 2000

TYPE OF REPORT: Annual

PREPARED FOR: U.S. Army Medical Research and Materiel Command
Fort Detrick, Maryland 21702-5012

DISTRIBUTION STATEMENT: Approved for Public Release;
Distribution Unlimited

The views, opinions and/or findings contained in this report are those of the author(s) and should not be construed as an official Department of the Army position, policy or decision unless so designated by other documentation.

FOREWORD

Opinions, interpretations, conclusions and recommendations are those of the author and are not necessarily endorsed by the U.S. Army.

<u>N/A</u> Where copyrighted material is quoted, permission has been obtained to use such material.

<u>N/A</u> Where material from documents designated for limited distribution is quoted, permission has been obtained to use the material.

<u>X</u> Citations of commercial organizations and trade names in this report do not constitute an official Department of Army endorsement or approval of the products or services of these organizations.

<u>N/A</u> In conducting research using animals, the investigator(s) adhered to the "Guide for the Care and Use of Laboratory Animals," prepared by the Committee on Care and use of Laboratory Animals of the Institute of Laboratory Resources, national Research Council (NIH Publication No. 86-23, Revised 1985).

<u>X</u> For the protection of human subjects, the investigator(s) adhered to policies of applicable Federal Law 45 CFR 46.

<u>N/A</u> In conducting research utilizing recombinant DNA technology, the investigator(s) adhered to current guidelines promulgated by the National Institutes of Health.

<u>N/A</u> In the conduct of research utilizing recombinant DNA, the investigator(s) adhered to the NIH Guidelines for Research Involving Recombinant DNA Molecules.

<u>N/A</u> In the conduct of research involving hazardous organisms, the investigator(s) adhered to the CDC-NIH Guide for Biosafety in Microbiological and Biomedical Laboratories.

Chan Hiang Ping   5/8/00
PI - Signature   Date

(4)   Table of Contents

(5)   Introduction

The goal of this proposed project is to develop a digital stereoscopic imaging technique for mammography. We hypothesize that stereoscopic imaging can be a practical technique with current detector and display technology and will improve the detection and analysis of breast lesions, especially for dense breasts. The improvement results from the facts that: (1) digital imaging systems generally can provide better contrast sensitivity for imaging dense tissues, (2) the overlying dense tissue will be separated from the lesion in the stereoscopic views thereby increasing the conspicuity of the lesion, and (3) the ability to analyze the 3-dimensional distributions and shapes of lesions such as calcifications and masses within the breast can potentially improve the accuracy of mammographic image interpretation by radiologists and reduce unnecessary biopsies.

To accomplish this goal, we will first develop an optimal imaging technique for acquisition of the stereoscopic images by using phantom studies. This includes the determination of the stereoscopic angle, the magnification factor, and the dose requirement in comparison with a single-image technique. To view the digital stereoscopic images, we will develop a stereoscopic viewing station with a high resolution graphics board and monitor and implement software for panning and roaming the displayed image. A stereoscopic viewer with an LCD shutter will be used to separate the left eye and right eye images. Any one image of the stereoscopic pair can also be read independently as in a conventional single-image reading condition. It is expected that this research will result in a practical digital stereoscopic imaging technique, which can improve the sensitivity of mammography for breast cancer detection, especially in dense breasts.

(6) Body

In the second year (4/20/99-4/19/00) of this grant, we have performed the following studies:

(A) Stereoscopic Viewing Station

As discussed in the first year report, we used a Neotek (Pittsburgh, PA) stereoscopic display system for our initial studies because that system was the only commercially available system that could be purchased with optional software to generate a virtual 3-D cursor. It would allow us to study the virtual cursor approach in the first year without waiting for our own software development. The Neotek system was capable of displaying only 1024 x 380 images. It used a synch-doubling stereoscopic mode of operation that required a reduction of the 1024 x 1024 resolution of the acquired images by more than a factor of 2. The displayed image quality was somewhat degraded. For the second year of our project, we purchased a high-resolution stereoscopic viewing station consisting of a Barco-Metheus (Beaverton, OR) model 1760S stereoscopic board with a SUN Microsystems (Palo Alto, CA) Ultra 10 computer. The Metheus board operates in a page flipping stereoscopic mode whereby the full left and right eye images are displayed sequentially, one after the other. This board is capable of displaying 1408 x 1408 x 8 bit stereo images at a refresh rate of 114 Hz on a high quality 21" Barco monitor. We viewed the stereo images with NuVision (Beaverton, OR) LCD stereoscopic glasses. The Metheus stereoscopic board came with very primitive display software. We have been developing our own software tools to add functionality to the workstation.

We developed an image display software package that includes lookup tables to display 12-bit and 8-bit input images, zoom and roam functions, image cropping, and contrast enhancement. Software was also written to allow the user to design and display virtual (stereoscopic) cursors and to display the x, y, and z positions of those cursors. The 3-D nature of the cursor is achieved by introducing offsets in the horizontal positions of the representations of the cursor in the left and right-eye images. The z-coordinate is equal to the offset. When the offset is 0, the cursor is at the same x, y position in both images, and it appears stereoscopically to be at the depth of the monitor screen. As the horizontal offset between the cursor positions is increased in one direction (e.g. left), the cursor appears to move closer to the observer, and as the offset is increased in the opposite direction (e.g. right), the cursor appears to move toward or into the monitor.

In order to make absolute depth measurements, the z-coordinate of the virtual cursor has to be calibrated. We have designed a calibration procedure as follows. We made a calibration phantom that contained thin wires placed on the steps of a stepwedge with known step heights. The stepwedge was imaged with a clinical Fischer MammoVision system in our Department. We used the same x-ray tube shifts as those employed for the stereo image acquisition of the phantoms employed in our observer studies. The wires that were utilized for calibration were oriented perpendicular to the tube shift direction. The resulting stereoscopic images were viewed without the stereo glasses and the left and right eye cursor positions were adjusted to overlay the left and right eye images of the wires on the steps. The z-coordinates of the cursor were linearly fit to the known depths of the wires to obtain the calibration line.

(B)   Improvement of a Stereoscopic Phantom for Depth Perception Study

We have designed a modular stereo phantom, which was improved this year. The phantom contains six 1-mm-thick Lexan sheets, each separated by spacers. Each Lexan plate contains a 5 X 5 array of object areas. Fifty nylon fibrils, each about 8 mm in length and 0.53 mm in diameter, are arranged in these object areas. Twenty-five fibrils are oriented vertically (perpendicular) and 25 horizontally (parallel) to the stereo shift direction. The fibrils are placed in the object areas on the six Lexan plates such that, in the projection image, each object area contains the projection of one vertical and one horizontal fibril that cross each other. On average, there are about 4 vertical and 4 horizontal fibrils on each plate. The depth separation of each pair of crossing fibrils depends on the arrangement of the plates and the thickness of the spacers. These plates can be randomly ordered to produce many independent object configurations. This new phantom is an improvement over our previous design in which one plate contained horizontal or vertical fibrils at each position (25 total on one plate), and each of the other plates contained far fewer fibrils.

(C)   Evaluation of the Effect of Virtual Cursor Shape on Depth Measurements in Digital Stereomammograms

In our study performed in the first year, we investigated the accuracies of observers' measurements of the depths of horizontally and vertically oriented nylon filaments that simulated fibrils in mammograms [ref. 1]. We found that with a cross-shaped virtual 3D cursor, observers could measure depths of vertically oriented fibrils to 1-2 mm, but their accuracies were degraded for horizontally oriented fibrils. During the second year, we performed a study to investigate whether the depth accuracy of the horizontally oriented fibrils might be improved through the use of a specially designed virtual cursor.

Observer Experiment

We employed the images that were generated for our previous investigation [ref. 1]. These images were obtained with the Fischer (Denver, CO) MammoVision Stereotaxic unit using a stereo x-ray tube shift angle of $-2.5°$ to $+2.5°$. The Fischer system acquires digital images of 1024 X 1024 pixels and 12 bit gray levels in a 5 cm X 5 cm field of view using a fiber-optics-coupled CCD detector. No antiscatter grid is used with the digital detector. The modular phantom described above was imaged with 1-mm thick spacers, resulting in depth separations of the fibrils from 2 to 10 mm. Two different phantom configurations were used. For the observer experiment, we had each participant use the stereoscopic virtual cursor system to measure the depths of 25 horizontally oriented fibrils in each of two images (two different phantom configurations) for a total of 50 depth measurements per person. Each participant made these measurements twice using different virtual cursors. One cursor was cross-shaped and the other was comb-shaped. The cursors are sketched in Figure 1, below.

The comb-shaped virtual cursor was chosen because it provides the observer with more vertical depth cues. It was hoped that when the observer positioned the comb cursor such that the horizontal fibril appeared to move through the central slot as the cursor depth was varied, the additional depth cues might assist the observer in locating the depth of the fibril.

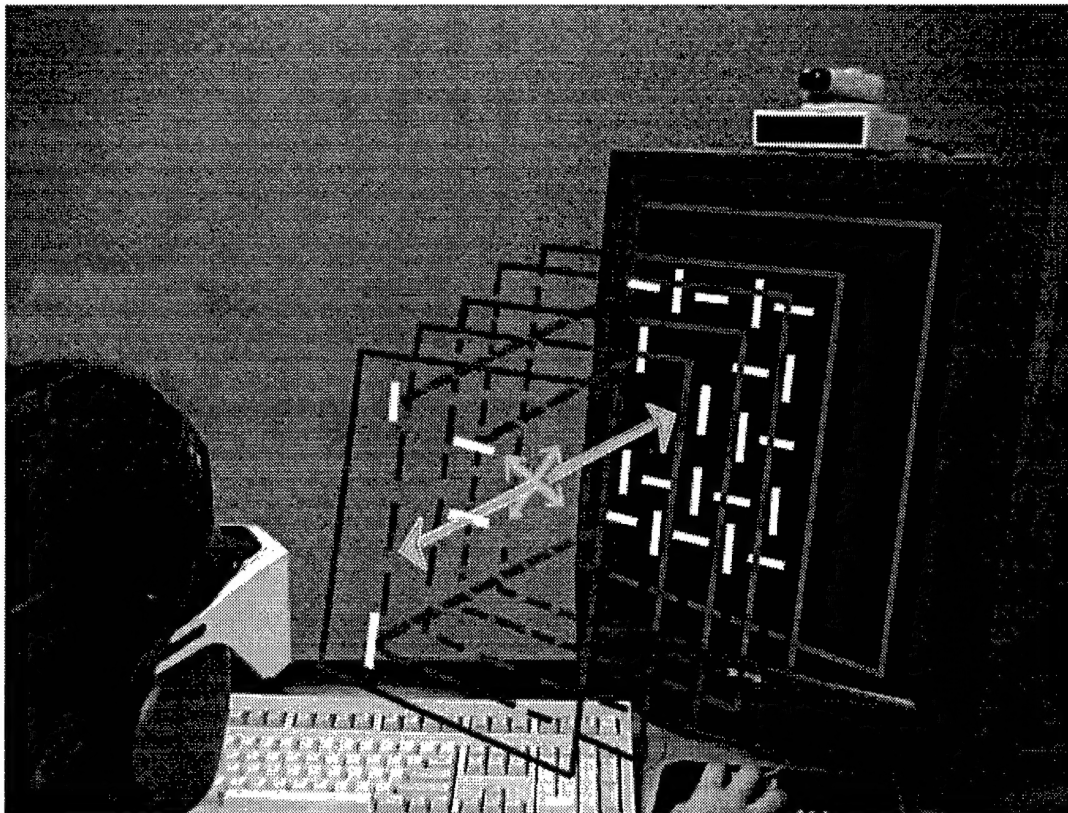Figure 1. "Cross-shaped" and "fan-shaped" virtual cursors employed in the experiment.

Figure 2. A graphical representation of the stereoscopic viewing system simulating the observer moving the virtual cursor within the stereo (3-D) image to match the horizontal fibril location.

An artist's interpretation of the stereoscopic viewing apparatus is shown in Figure 2. The observers recorded their measured z-coordinates of each horizontally oriented fibril, and these z-coordinates were converted to depths using the calibration line that was calculated from the stepwedge data discussed above. These depths were then compared with the known depths in terms of the parameters associated with least-square linear fits (slope, intercept, correlation coefficient (r-value), and standard error of the estimate (SEE)) of the measured depths to the true depths and in terms of the root mean square (RMS) errors of the measurements. The latter were computed using the equation:

$$RMS\ error = \sqrt{\frac{\sum_{i=1}^{50}(true\ depth_i - measured\ depth_i)^2}{50}}$$

Results

Table 1. Linear fit parameters and RMS errors for measured vs. true depths of horizontally oriented fibrils.

	Observer 1	Observer 1 Repeat	Observer 2	Observer 3	Observer 4
Slope (cross)	0.71	0.74	1.02	0.48	0.56
Slope (comb)	0.91	0.94	0.87	0.51	0.47
Intercept (cross)	0.44	1.09	-0.50	0.04	1.54
Intercept (comb)	0.79	0.63	0.75	1.94	1.11
r-value (cross)	0.80	0.83	0.94	0.55	0.48
r-value (comb)	0.98	0.97	0.95	0.60	0.49
SEE (cross) mm	1.70	1.58	1.20	2.32	3.28
SEE (comb) mm	0.64	0.72	0.95	2.16	2.68
RMS error (cross) mm	2.17	1.76	1.24	3.84	3.57
RMS error (comb) mm	0.76	0.80	0.98	2.68	3.50

The results of the experiment are summarized in Table 1 and Figure 3. In this experiment, we found that depth measurements made with the new comb-shaped cursor were more accurate. The RMS errors in the observers' measurements improved by 0.1 to 1.4 mm with this cursor relative to the cross-shaped cursor. In fact, with this new cursor, two of the observers were able to measure the depths of the horizontally oriented fibrils to an accuracy of about 1 mm, which approaches their accuracies for the vertically oriented fibrils in our previous study [ref. 1]. One of the observers repeated the entire experiment twice and those results appear in Table 1 above. The linear fit parameters and RMS errors for the two trials by the same observer are very similar, indicating the results for that observer are very reproducible.
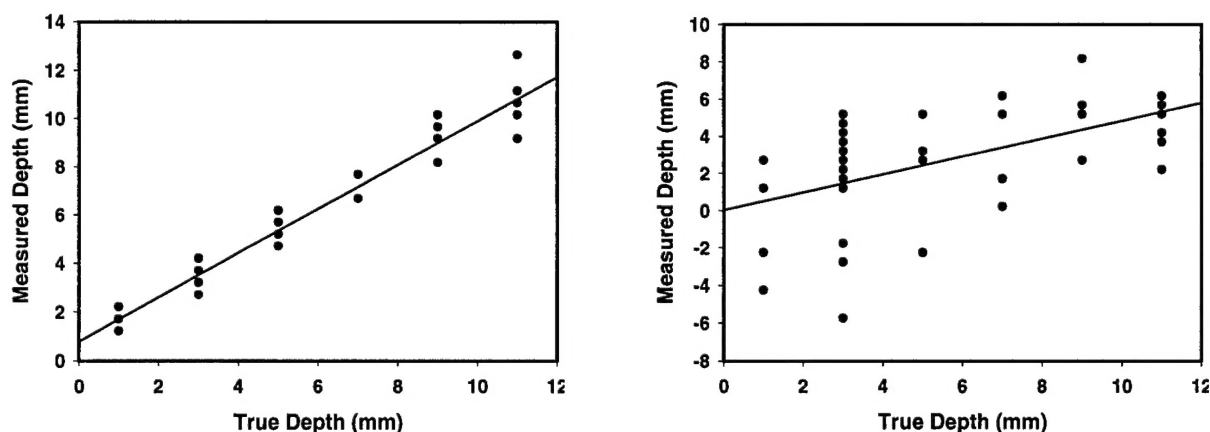
Figure 3. Left: Best measured vs. true depth result (observer #1, comb cursor)
Right: Worst measured vs. true depth result (observer #3, cross cursor)

The accuracies of all of the observers' measurements that are listed in Table 1 do not tell the whole story, however. They do not reflect the amount of time required to make the measurements. In general, observers spent much more time locating the positions of the horizontally oriented fibrils as compared with the vertically oriented fibrils. The observers would move the cursors in and out several times to hone in on the depths, which were much less obvious than the depths of the vertically oriented fibrils. The good results that were obtained indicate that the extra time and effort were worthwhile. Most objects in mammograms have orientations that are between horizontal and vertical, and even small vertical components make the depths easier to visualize and help reduce measurement times. We have designed an anthropomorphic breast phantom containing spiculated masses and microcalcification clusters at various known depths. In future studies, we will analyze the accuracies of depth measurements of the spiculations, microcalcifications and masses in that phantom with virtual cursors of different shapes and sizes.

(D)   Effects of Stereoscopic Imaging Techniques on Depth Discrimination

The second major study that was performed during the second year of this project was an investigation of the dependence of depth discrimination on stereoscopic shift and x-ray exposure. Digital stereoscopic image pairs were acquired with the Fischer Mammotest stereotaxic prone biopsy table. For this system, the automatic exposure technique at 26 kVp for a 4.2-cm-thick Lucite phantom is about 160 mAs. To simulate the attenuation and scatter conditions of imaging an average breast, the fibril phantom described above was sandwiched between two 2-cm-thick slabs of BR-12 breast tissue simulating plastic. We acquired stereoscopic pairs of images at ±2.5° and ±5° stereo-angles using 26 kVp and 40, 70, 140 mAs per image. Three different configurations of the fibril phantom were imaged under each exposure condition, producing 75 pairs of fibril images at 5 different depth separations under each condition. A training image of the fibril phantom without the 4 cm of BR-12 was also acquired at 26 kVp and 10 mAs. .

Observer Experiment

Nine observers participated in the experiment. A total of 18 stereoscopic image pairs (2 stereo-angles X 3 exposure levels X 3 phantom configurations) were viewed by each observer. Each image contained 25 crossing pairs of fibrils separated by one of five different spacings (2, 4, 6, 8, 10 mm). The observer was asked to visually judge if the vertical fibril in each pair of overlapping fibrils was in front of or behind the horizontal fibril. Each observer read the 18 images sequentially in a different pre-assigned randomized order. The reading orders of the observers were chosen so that, on average, no image acquired under a specific condition would be read more frequently in a certain order. This minimized the effects of observer learning, memorization, or fatigue on the reading results. The observer was not informed of the conditions under which the image being viewed was acquired. The training image was read before the experiment by each observer to familiarize him or her with the reading task.
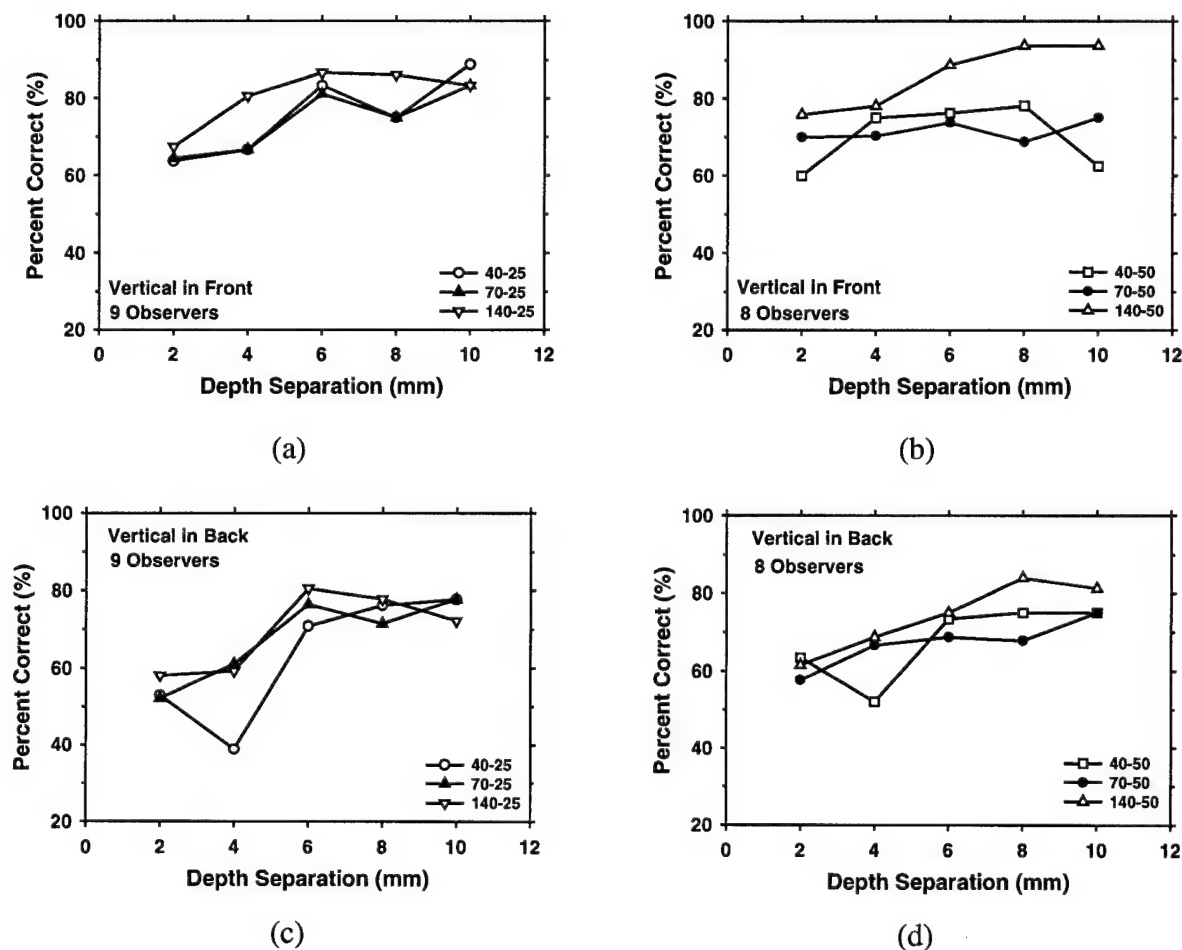
Results

Figure 4. Dependence of percentage of correct decisions, averaged over 9 ($\pm2.5°$) or 8 ($\pm5°$) observers, on depth separation and imaging conditions: (a) vertical fibril in front, $\pm2.5°$ stereo-angle, (b) vertical fibril in front, $\pm5°$ stereo-angle, (c) vertical fibril in back,

±2.5° stereo-angle, and (d) vertical fibril in back, ±5° stereo-angle. 40 mAs, 70 mAs, 140 mAs were used for image acquisition.

It was found that the stereovision acuity of the observers differed by a wide range and it appeared to depend on the quality of the stereoscopic images. All observers could perceive the stereoscopic training image with reasonable accuracy in judging the relative depths of the crossing fibrils. The fibrils in the training image had a higher contrast and signal-to-noise ratio than the test images. It was acquired without the 4 cm BR-12 phantom so that the scattered radiation was much lower than that in the test images. Some observers found it much more difficult to merge the left-eye and right-eye images to achieve a stereoscopic effect when they viewed the test images. This occurred more often with the images acquired at ±5° stereo-angle than those acquired at ±2.5° stereo-angle. One of the observers failed to merge the images at the ±5° stereo-angle so that the results at this angle were analyzed for only 8 observers.

Figures 4(a)-(d) show the percentages of correct decisions plotted as a function of the depth separation of the crossing fibrils, averaged over 9 (±2.5°) or 8 (±5°) observers, for the different imaging conditions studied. Because of the large variation in the accuracy of the observers, the standard deviations of the mean were large, ranging from 4% to 13%. The differences in the percentages of correct decisions between the different conditions were therefore not statistically significant. However, some trends can be observed. The curve for the highest exposure, 140 mAs, tended to be slightly higher than those for the other two exposures, except for a few points. The 140 mAs curves were also smoother than the other curves, indicating less variability in the readings. At this exposure level, the percentages of correct decisions appeared to increase by about 15 to 20% as the depth separation increased from 2 mm to 10 mm, and increase by an average of about 5% as the stereo-angle increased from ±2.5° to ±5°, when other conditions were fixed. The percentages of correct decisions were 10 to 15% higher when the vertical fibrils were in front of the horizontal fibrils than when they were in the back.

Three of the observers had a higher accuracy in depth discrimination than the others. On average, their percentages of correct decisions were about 10% to 20% higher than the other 6 observers under most conditions, and were 40% to 50% higher in some cases. For these observers, it is more obvious that the accuracy was higher when the vertical fibrils were in front of the horizontal fibrils. For the smallest fibril separation of 2 mm, the accuracy was about 20% higher when the vertical fibril was in the front.

This study shows that depth discrimination in stereomammography depends on imaging conditions and object configurations. For viewing of fibrils that simulated spiculations or thin fibrous structures in mammographic images, the accuracy of depth discrimination appeared to increase with increasing exposure and stereo-angle. However, many observers found it difficult to merge the left-eye and right-eye images acquired with a large stereo-shift to achieve stereovision. Further studies will be conducted to evaluate the depth perception of different mammographic test objects.

(7)   Key Research Accomplishments

- Develop software for image display and manipulation on a high-resolution stereoscopic viewing station

- Develop software for generating 3D virtual cursors on stereoscopic display

- Perform observer experiment to study the effects of 3D virtual cursors shape on depth measurements in digital stereomammograms

- Perform observer experiment to study the effects of stereoscopic imaging techniques on depth discrimination

(8)   Reportable Outcomes

As a result of the support by the BCRP grant, we have conducted extensive studies in stereomammography and have presented results in a conference, and will report further work in one journal article and two additional conference presentations and proceedings. The results will also be reported at the Era of Hope meeting to be held in June this year at Atlanta, Georgia.

Journal Articles Accepted for Publication:

Goodsitt MM, Chan HP, Hadjiiski LM. Stereomammography: Evaluation of depth perception using a virtual 3D cursor. Medical Physics (in press).

Conference Presentation and Proceedings

1. Goodsitt MM, Chan HP, Hadjiiski LM. Stereomammography: Evaluation of Depth Perception using a Virtual 3D Cursor. Presented at the 85th Scientific Assembly and Annual Meeting of the Radiological Society of North America, Chicago, IL, November 28-December 3, 1999. Radiology 1999; 213(P): 368.

2. Goodsitt MM, Chan HP, Sullivan JM, Darner KL, Hadjiiski LM. Evaluation of the Effect of Virtual cursor shape on depth measurements in digital stereomammograms. Accepted for presentation at The 5th International Workshop on Digital Mammography. IWDM-2000. Toronto, Canada. June 11-14, 2000. *Proceeding of The 5th International Workshop on Digital Mammography* (in press).

3. Chan HP, Goodsitt MM, Darner KL, Sullivan JM, Hadjiiski LM, Petrick N, Sahiner B. Effects of stereoscopic imaging technique on depth discrimination. Accepted for presentation at The 5th International Workshop on Digital Mammography. IWDM-2000. Toronto, Canada. June 11-14, 2000. *Proceeding of The 5th International Workshop on Digital Mammography* (in press).

4. Chan HP, Goodsitt MM., Sullivan JM, Darner KL, Hadjiiski LM. Depth perception in digital stereoscopic mammography. Accepted for presentation at the Era of Hope Meeting, U. S.

Army Medical Research and Materiel Command, Department of Defense, Breast Cancer Research Program, Atlanta, Georgia, June 8-12, 2000.

(9) Conclusions

During this year, we have assembled a high-resolution stereoscopic viewing station and developed software for displaying and manipulating stereoscopic images. This viewing station facilitates our studies of various image acquisition and display techniques for stereoscopic imaging. Various 3D virtual cursor shapes were studied and two were chosen for an observer study to evaluate their effects on depth measurement. An observer study was also performed to study the effects of imaging techniques (x-ray dose and stereo-angles) on depth perception. The results of these experiments indicate that the 3D virtual cursors can provide absolute measurement of lesion (in particular, fibril) size and depth in the breast. The accuracy of the measurements depends on matching of the object shape and cursor shape. It was also found that depth perception depends on the quality of the stereo-images. This information is important for designing optimal imaging techniques to generate stereomammograms and for designing proper 3D virtual cursors to quantify lesion size and depth in stereomammograms. The improvement in perception of the details of mammographic features and the additional size and depth information are expected to improve diagnostic accuracy of mammographic abnormalities.

(10) References

1. Goodsitt MM, Chan HP, Hadjiiski LM. Stereomammography: Evaluation of depth perception using a virtual 3D cursor. Medical Physics (in press).

(11) Appendix

Copies of the following publications are enclosed with this report:

Journal Article

Goodsitt MM, Chan HP, Hadjiiski LM. Stereomammography: Evaluation of depth perception using a virtual 3D cursor. Medical Physics (in press).

Conference Proceedings and Abstract

1. Goodsitt MM, Chan HP, Hadjiiski LM. Stereomammography: Evaluation of Depth Perception using a Virtual 3D Cursor. Presented at the 85th Scientific Assembly and Annual Meeting of the Radiological Society of North America, Chicago, IL, November 28-December 3, 1999. Radiology 1999; 213(P): 368.

2. Goodsitt MM, Chan HP, Sullivan JM, Darner KL, Hadjiiski LM. Evaluation of the Effect of Virtual cursor shape on depth measurements in digital stereomammograms. In: *Proceeding*

of The 5th International Workshop on Digital Mammography. IWDM-2000. Toronto, Canada. June 11-14, 2000 (in press).

3. Chan HP, Goodsitt MM, Darner KL, Sullivan JM, Hadjiiski LM, Petrick N, Sahiner B. Effects of stereoscopic imaging technique on depth discrimination. In: *Proceeding of The 5th International Workshop on Digital Mammography.* IWDM-2000. Toronto, Canada. June 11-14, 2000 (in press).

4. Chan HP, Goodsitt MM., Sullivan JM, Darner KL, Hadjiiski LM. Depth perception in digital stereoscopic mammography. Abstract in the *Proceeding of the Era of Hope Meeting*, U. S. Army Medical Research and Materiel Command, Department of Defense, Breast Cancer Research Program, Atlanta, Georgia, June 8-12, 2000 (in press).

Stereomammography: Evaluation of Depth Perception Using a Virtual 3D Cursor

Mitchell M. Goodsitt, Ph.D., Heang-Ping Chan, Ph.D., and Lubomir Hadjiiski, Ph.D.

Department of Radiology

University of Michigan

Ann Arbor, MI 48109-0030

Corresponding Author: Mitchell M. Goodsitt, Ph.D.
Department of Radiology
University of Michigan Hospitals
Room B1 F510C
1500 East Medical Center Drive
Ann Arbor, MI   48109-0030

Office: 734-936-7474
FAX: 734-936-7948
E-mail: goodsitt@umich.edu

ABSTRACT

We are evaluating the usefulness of stereomammography in improving breast cancer diagnosis. One area that we are investigating is whether the improved depth perception associated with stereomammography might be significantly enhanced with the use of a virtual 3-D cursor. A study was performed to evaluate the accuracy of absolute depth measurements made in stereomammograms with such a cursor. A biopsy unit was used to produce digital stereo images of a phantom containing 50 low contrast fibrils (0.5-mm diameter monofilaments) at depths ranging from 0 to 10 mm, with a minimum spacing of 2 mm. Half of the fibrils were oriented perpendicular (vertical) and half parallel (horizontal) to the stereo shift direction. The depth and orientation of each fibril were randomized, and the horizontal and vertical fibrils crossed, simulating overlapping structures in a breast image. Left and right eye images were generated by shifting the x-ray tube from $+2.5°$ to $-2.5°$ relative to the image receptor. Three observers viewed these images on a computer display with stereo glasses and adjusted the position of a cross-shaped virtual cursor to best match the perceived location of each fibril. The x, y and z positions of the cursor were indicated on the display. The z (depth) coordinate was separately calibrated using known positions of fibrils in the phantom. The observers analyzed images of two configurations of the phantom. Thus, each observer made 50 vertical filament depth measurements and 50 horizontal filament depth measurements. These measurements were compared with the true depths. The correlation coefficients between the measured and true depths of the vertically oriented fibrils for the 3 observers were 0.99, 0.97, and 0.89 with standard errors of the estimates of 0.39 mm, 0.83 mm, and 1.33 mm, respectively. Corresponding values for the horizontally oriented fibrils were

0.91, 0.28, and 0.08, and 1.87 mm, 4.19 mm, and 3.13 mm. All observers could estimate the absolute depths of vertically oriented objects fairly accurately in digital stereomammograms; however, only one observer was able to accurately estimate the depths of horizontally oriented objects. This may relate to different aptitudes for stereoscopic visualization. The orientations of most objects in actual mammograms are combinations of horizontal and vertical. Further studies are planned to evaluate absolute depth measurements of fibrils oriented at various intermediate angles and of objects of different shapes. The effects of the shape and contrast of the virtual cursor and the stereo shift angle on the accuracy of the depth measurements will also be investigated.

Key words: stereomammography, stereoscopic, virtual cursor, 3-dimensional

I. INTRODUCTION

Presently, screening x-ray mammography is the only technique that has a proven capability for detecting early stage clinically occult cancers.[1] Although mammography has a high sensitivity for detecting breast cancers, studies have shown that radiologists do not detect all carcinomas that are visible on retrospective analyses of the mammograms.[2-11] These missed detections are often a result of the very subtle nature of the mammographic findings. One of the major deficiencies of mammography is the inability to discern masses and microcalcifications hidden in dense fibroglandular tissue.[12] It is estimated that about 20% of the breast cancer in dense breasts are not detected by mammography.[9,11] Conventional mammography is a two-dimensional projection image of a 3-dimensional structure. As a result, objects along the same x-ray beam path overlap each other. The overlying tissue structures often obscure the visibility of subtle lesions of interest in the mammogram. The camouflaging of the anatomical structures is the main cause of missed diagnoses. Overlapping structures can also project onto the image plane forming shadows that appear to be lesions, resulting in false positive findings. Radiologists examine two or more projections of each breast to improve their ability to detect lesions and to assist them in distinguishing between true lesions and overlapping tissues. However, standard mammographic techniques are not always successful in distinguishing true lesions from overlapping tissues. Digital stereomammography is a method that could potentially solve many of these problems.

Stereomammography is not a new technique. It was first described in 1930.[13] Like other forms of stereoradiography at that time, it involved taking two film images, a left eye image and a right eye image. These were obtained by positioning the x-ray tube

at a certain distance to the left and to the right of the central axis. Usually, the total tube shift was 10% of the source-to-image distance.[14] The radiologist would view the images using a cross-eyed technique or a special stereoscopic viewer.[14] Stereoradiography and stereomammography lost favor because of the increased radiation dose, procedure time, and film costs associated with taking two radiographs, and because it generally took more time to read stereoradiographs. According to Christensen's Physics of Diagnostic Radiology [14], another reason for reduced use of stereoradiography was radiologists' disappointment with the technique because they failed to appreciate the fact that stereoradiography did not enable them to accurately judge the distances between objects. Rather, stereoradiography allowed for relative depth perception, whereby one could "accurately rank objects in their order of closeness." [14]

The advent of digital imaging techniques and video image displays has made stereoradiography and stereomammography attractive again. Research has been performed in digital stereoangiography[15-17] and digital stereomammography.[18,19] Furthermore, stereotaxic techniques have been developed for core biopsies of breast lesions. In stereotaxic breast biopsies, much larger stereo angles ($+15^\circ$ to the right and -15° to the left) are employed, compared to the angles used in stereoscopic visualization. These larger angles result in increased parallax ("the apparent displacement of an object when viewed from two different vantage points" [14]) which in turn permits more accurate depth determination. With stereotaxic techniques, the operator identifies the location of the lesion in each image, and a computer calculates the spatial coordinates (x, y, and z (depth)) of the lesion using equations derived from simple geometry.[20] For example the distance of the lesion from a fixed image receptor is given by the equation

$$z_l = x_{ls} / (2 \tan(15^\circ)),$$

where x_{ls} is the parallax shift of the lesion on the image receptor.[20]

This capacity to measure absolute depths contradicts the relative depth perception limitation of stereoradiography mentioned by Christensen, and in considering this, we conceived the idea of using a virtual (3-D) cursor to determine the positions of lesions within a stereoscopic image. The proposed virtual cursor would be calibrated in the x, y, and z directions and would be displayed and moved within the stereoscopic image. To our knowledge, such a cursor has never been developed or used in stereoradiography. We performed a literature search and did find that stereographic cursors or pointers have been developed and tested for other purposes, especially for computer graphics and for the operation of robots in remote environments.[21-24] The application of these cursors to x-ray images as opposed to video or computer graphic images is quite different because x-ray images result from transmission rather than reflection and therefore have a more cloud-like, transparent/translucent quality. Furthermore, additional depth cues due to perspective (closer objects appearing larger than distant objects), occlusion (closer objects obscuring distant objects), shadows (in particular, interactive shadows that move as the objects' positions change) and texture (closer objects having more distinct surface features)[25] are not apparent in radiographs.

The purpose of the present paper is to describe a proof-of-concept study that we performed using a virtual cursor in stereomammography images to determine the depths of selected objects.

3

II. METHODS

A. Phantom

The phantom that was employed to evaluate the depth accuracy of measurements made with the virtual cursor consisted of six 10 cm x 10 cm sheets of 1-mm-thick Lexan separated by 1-mm-thick spacers placed at the corners of each sheet. The test objects were 8-mm long, 0.53-mm diameter fibrils (nylon monofilaments (e.g., fish line)), which simulated low contrast spiculations in mammograms. The fibrils were positioned within a 4.5-cm x 4.5-cm central region of the Lexan sheets. A total of 50 fibrils were taped to the sheets with 25 oriented perpendicular (vertical) and 25 oriented parallel (horizontal) to the stereo shift direction. The depth and orientation of each fibril were randomized, and the horizontal and vertical fibrils crossed simulating overlapping structures in a breast image. The end result was a 5 x 5 array of crossed (horizontal and vertical) filaments, each of which could be examined for its depth. (See Figure 1.) With this arrangement, the minimum depth difference between the fibrils was 2-mm and the maximum was 10-mm. The order of the six Lexan layers could be varied to create many independent phantom configurations for analysis by each reader. In this study, two configurations were randomly chosen.

B. Stereo image acquisition

The phantom was imaged with a Fischer (Denver, CO) MammoVision Stereotaxic unit. According to Christensen's Physics of Diagnostic Radiology[14], early

4

radiologists learned by "trial and error that a tube shift equal to 10% of the target-film distance produced satisfactory results." [14]   This tube shift is equal to a total stereo-shift angle of about 6 degrees (e.g. $+3^{o}$ and -3° relative to a line perpendicular to the image receptor.)   In general, larger tube shifts produce improved depth perception, but beyond a certain limit, this is achieved at the expense of increased observer fatigue[26] and decreased stereo field of view. The angle scale on the Fischer unit is marked in 5 degree increments, and our preliminary investigations with the Fischer digital system indicated a stereo shift of $+2.5^{o}$ to -2.5^{o} produced images that appeared to have adequate depth discrimination without producing undue eyestrain. This stereo angle was therefore used for image acquisition in this study. It corresponds with a total stereo shift of about 9% (5.94 cm) for the 68 cm source-to-image distance of the Fischer system. Future studies will be performed to determine the optimal angle for accurate depth perception with acceptable eyestrain. The Fischer unit has a fiber- optic-coupled CCD detector that produces 1024 x 1024 x 12-bit images.   The images can be stored in 1024 x 1024 x 8-bit TIFF format or transmitted to a DICOM server. We employed the TIFF formatted images in this study. Since no contrast enhancement was performed on the displayed images in the observer study, it is unlikely that a bit depth greater than 8-bits could have been perceived in the displayed images. Therefore, it is unlikely that compression to 8-bits influenced our results.

C. Stereoscopic viewer and virtual cursor

The images were displayed on a personal computer using a Model SS-03 Stereo Display Processor from Neotek, Inc. (Pittsburgh, PA). We used Neotek's Composer software to format the images and their optional Presenter software to display the images along with a virtual cursor. The Presenter software also generates a display of the x, y, and z- positions of the virtual cursor. The Neotek system produces stereo images via a method termed "synch-doubling." In this method, the left eye image is stored above the right eye image in the video graphics board (see Figure 2), and an additional vertical synch pulse is inserted between the two images in the video signal coming from the computer. This synch-doubling causes the images to be displayed fully on the monitor at twice the normal refresh rate for reduced flicker (i.e., if the board is run at a 60 Hz refresh rate, the images are displayed at 120 Hz). The graphics board was operated in the 1024 (horizontal) x 768 (vertical) resolution mode recommended by Neotek. The Neotek Composer software downsized the 1024 x 1024 images to fit two images (the left on top of the right) within this resolution. That is, it converted the left and right eye images to each be about 1024 x 340. The loss in vertical resolution was necessitated by the synch-doubling. It had minimal effect in this study since the stereo shift direction corresponding with the horizontal display direction.

6

D. Observer study

Three observers (two medical physicists and a computer scientist) viewed the images on the computer monitor with a pair of Neotek stereo glasses. These employ LCD shutters that are synchronized with the display to allow viewing of the left image by the left eye and the right image by the right eye. The observers used the up and down arrow keys on the computer keyboard to adjust the position of a cross-shaped virtual cursor to best match the perceived location of each fibril, and noted the z (depth) coordinates on a data sheet.

The z-coordinate was separately calibrated using the known positions of fibrils in the phantom. This was accomplished by viewing the images without the stereo glasses (see Fig. 2) and adjusting the left and right eye cursors to overlay the left and right eye representations of the vertical fibrils in the two images. The z-coordinates of the cursor were linearly fit to the known positions to obtain a calibration line.

Each observer analyzed images of two configurations of the phantom. Thus, each observer made 50 vertical filament depth measurements and 50 horizontal filament depth measurements. Linear least-square fits were performed to compare the measurements with the true depths.

III. RESULTS

Table I lists the slopes, intercepts, correlation coefficients (r-values) and standard errors of the estimates (SEE) of the least squares fits to the depth measurements made by

7

the readers in each of the two images that they examined. The results in this table are separated into those for the vertically and horizontally oriented fibrils. Plots of the best and worst results in terms of the standard errors of the estimates are displayed in Figures 3 and 4. Computed root mean square (RMS) errors for the fibril measurements are listed in Table II.

IV. DISCUSSION

All observers could estimate the absolute depths of the vertically oriented objects fairly accurately in digital stereomammograms; however, only one observer was able to accurately estimate the depths of the horizontally oriented objects. For the vertically oriented fibrils, the overall average r-value was 0.949 and SEE was 0.85 mm. The RMS errors in the depth measurements ranged from 0.6 mm to 1.9 mm with an average value for all 3 readers of 1.2 mm. These RMS errors indicate that the absolute measurements with the virtual cursor are accurate to within 2 mm. This is consistent with relative stereoscopic studies performed by Doi and Duda[26] and Higashida et al[15] and absolute stereoscopic studies performed by Fencil et al[16]. Doi and Duda and Higashida et al investigated observers' abilities to distinguish (as opposed to measure) the separation of objects that were superimposed on stepwedge phantoms. In Doi and Duda's study[26], the objects were 0.2-mm diameter aluminum wires. A matrix of "plus" objects were formed by placing horizontally and vertically oriented pieces of wire at the bottom of the stepwedge, with their counterparts located directly above on the step of known thickness (e.g. horizontal wire on step if bottom wire is vertical). The "plus" objects were imaged

8

stereoscopically using a geometric magnification factor of 2 and x-ray focal spot shifts of 1.25%, 2.5% and 5% of the focus-to-film distance. These investigators found that observers could correctly identify 1-mm separations between two aluminum wires 80% of the time for the 5% tube shift and between 60 and 70% for the other tube shifts. In Hagashida et al's study[15], a similar phantom was used. Teflon tube objects filled with contrast media were arranged on the stepwedge to form cross (or 'x') shaped objects. They employed a geometric magnification factor of 1.1 and the x-ray focal spot shift for stereoscopic imaging was 6.5% of the focus-to-image intensifier distance. They found that observers could correctly identify 1.6-mm separations between 1-mm diameter tubes containing 25% iodine contrast more than 80 % of the time.

Our study and results can be distinguished from those of Doi and Duda[26] and Higashida et al[15] because we investigated absolute rather than relative stereoscopic measurements and because we analyzed horizontally and vertically oriented objects separately. With respect to absolute measurements, Fencil et al[16] imaged a box phantom containing aluminum wires that simulated blood vessels at different angles. Fencil et al employed an automated cross-correlation technique to determine the position of a wire (vessel) segment in the second image of a stereoscopic pair after it was selected in the first image. They obtained an average calculated distance error of approximately +/- 2 mm, which is similar to our error for vertically oriented fibrils and the errors in the studies of Doi and Duda and Higashida et al that are cited above. Our technique is easier to implement than Fencil et al's, but more observer dependent, as the observer effectively judges the correlation between the cursor and the fibrils in both images of the stereoscopic pair.

The fact that the observers in our study did worse at measuring the depths of horizontally as opposed to vertically oriented fibrils is not surprising since the image discrepancy and hence the stereoscopic effect is less for the horizontal objects (i.e., there is considerable overlap between corresponding horizontally oriented objects in the stereo pairs, and the shifts in positions are not as apparent).[14] There appears to be a larger difference in the performance among the observers for the horizontally oriented fibrils, with one observer performing very well and the other two very poorly. This may be related to different aptitudes for stereoscopic visualization.

The orientations of most objects in actual mammograms are combinations of horizontal and vertical. Further studies are planned to evaluate absolute depth measurements of fibrils oriented at various intermediate angles and of objects of different shapes. The effects of the shape and contrast of the virtual cursor and of the stereo shift angle on the accuracy of the depth measurements will also be investigated. Finally, the cursors will be applied to digital stereomammograms of breast biopsy samples to determine their applicability in estimating lesion depths and dimensions and in providing additional depth cues for improved stereoscopic image interpretation.

ACKNOWLEDGMENTS

10

REFERENCES

1. H. Seidman, S. K. Gelb, E. Silverberg, N. LaVerda and J. A. Lubera, "Survival experience in the Breast Cancer Detection Demonstration Project," CA Cancer J Clin. 37, 258-290 (1987).

2. M. Moskowitz, *Benefit and Risk. In: Breast Cancer Detection: Mammography and Other Methods in Breast Imaging*, 2nd ed. Eds. L. W. Bassett and R. H. Gold, (Grune and Stratton, New York, 1987).

3. J. E. Martin, M. Moskowitz, and J. R. Milbrath, "Breast cancer missed by mammography," AJR 132, 737-739 (1979).

4. B. J. Hillman, L. L. Fajardo, T. B. Hunter et al, "Mammogram interpretation by physician assistants," AJR 149, 907-911 (1987).

5. L. Kalisher, "Factors influencing false negative rates in xeromammography," Radiology 133, 297-301 (1979).

6. L. W. Bassett, D. H. Bunnell, R. Jahanshahi, R. H. Gold, R. D. Arndt, and J. Linsman, "Breast cancer detection: one versus two views," Radiology 165, 95-97 (1987).

7. C. J. Baines, A. B. Miller, C. Wall et al, "Sensitivity and specificity of first screen mammography in the Canadian National Breast Screening Study: A preliminary report from five centers," Radiology 160, 295-298 (1986).

8. P. J. Haug, I. M. Tocino, P. D. Clayton, and T. L. Bair, "Automated management of screening and diagnostic mammography," Radiology 164, 747-752 (1987).

9. M. G. Wallis, M. T. Walsh, and J. R. Lee, "A review of false negative mammography in a symptomatic population," Clinical Radiology 44, 13-15 (1991).

10. J. A. Harvey, L. L. Fajardo, and C. A. Innis, "Previous mammograms in patients with impalpable breast carcinomas: Retrospective vs blinded interpretation," AJR 161, 1167-1172 (1993).

11. R. E. Bird, T. W. Wallace, and B. C. Yankaskas, "Analysis of cancers missed at screening mammography," Radiology 184, 613-617 (1992).

12. V. P. Jackson, R. E. Hendrick, S. A. Feig, and D. B. Kopans, "Imaging of the radiographically dense breast," Radiology 188, 297-301 (1993).

13. S. L. Warren , "Roentgenologic study of the breast," AJR 24, 113-124 (1930).

14. T .S. Curry, J. E. Dowdey, and R. C. Murry. *Christensen's Physics of Diagnostic Radiology*, 4th Edition (Lea & Febiger, Philadelphia, PA, 1990).

15. Y. Higashida, Y. Hirata, R. Saito, S. Doudajuki, H. Bussaka, and M. Takahashi, "Depth determination on sterescopic digital subtraction angiograms," Radiology 168, 560-562 (1988)

16. L. E. Fencil, K. Doi, and K. R. Hoffman, "Accurate analysis of blood vessel sizes and stenotic lesions using stereoscopic DSA system," Invest Radiol 23, 33-41 (1988)

17. T. Moll, P. Douek, G. Finet, F. Turjman, C. Picard, D. Revel, and M. Amiel, "Clinical assessment of a new stereoscopic digital angiography system," Cardiovascular and Interventional Radiology 21, 11-16 (1998)

18. J. Hsu, D. M. Chelberg, C. F. Babbs, Z. Pizlo, and E. Delp, "Pre-clinical ROC studies of digital stereomammography," IEEE Trans Med Imaging 14, 318-327 (1995)

19. D. Getty, "Stereoscopic digital mammography: Improving diagnostic accuracy," Technology Transfer Workshop on Breast Cancer Detection, Diagnosis, and Treatment, May 1-2, 1997, Washington, D. C., (1997).

20. R. E. Hendrick and S. H. Parker, "Stereotaxic Imaging," in *Syllabus: A Categorical Course in Physics Technical Aspects of Breast Imaging*, Third Edition (Radiological Society of North America, Inc, Northbrook, IL, 1994) pp. 263-274.

21. D. R. W. Butts and D. F. McAllister, "Implementation of true 3D cursors in computer graphics," SPIE Vol 902. Three-dimensional imaging and Remote Sensing Imaging, 74-82 (1988)

22. F. W. Reinhardt, *Effects of Depth Cues on Judgements Using a Field-Sequential Stereoscopic CRT Display*, Ph.D. dissertation, Industrial Engineering and Operations Research Dept, Virginia Polytechnic Institute & State University, 1990

23. Y. Y. Yeh and L. D. Silverstein, "Depth discrimination in stereoscopic displays," SID '89 Digest, 372-375 (1989).

24. D Drascic and P Milgram, "Positioning accuracy of a virtual stereographic pointer in a real stereoscopic video world," SPIE volume 1457: Stereoscopic displays and Applications II, 58-69 (1991).

25. S Zhai, W Buxton, and P Milgram, "The partial occlusion effect: Utilizing semi-transparency in 3D human computer interaction, Proc CHI'94, ACM Conf on Human Factors in Computing Systems, April, 1994, Boston, MA, (1994).

26. K Doi and E. E. Duda, "Detectability of depth information by use of magnification stereoscopic technique in cerebral angiography," Radiology, 146, 91-95 (1983).

Table I. Linear regression results for measured vs. true depths in phantom images

A) Vertically oriented fibrils

Reader	Image	slope	intercept	r-value	SEE (mm)
A	1	1.025	-0.56	0.992	0.39
A	2	1.017	-0.56	0.994	0.38
Average A				0.993	0.39
B	1	0.845	-0.65	0.887	1.33
B	2	0.868	-0.61	0.891	1.32
Average B				0.889	1.33
C	1	1.087	-1.62	0.963	0.92
C	2	0.955	0.00	0.968	0.74
Average C				0.966	0.83
Overall Average		0.966	-0.67	0.949	0.85

B) Horizontally oriented fibrils

Reader	Image	slope	intercept	r-value	SEE (mm)
A	1	1.129	-3.04	0.947	1.24
A	2	1.135	-4.66	0.871	2.50
Average A				0.909	1.87
B	1	0.003	-5.57	0.004	2.55
B	2	0.176	-7.52	0.154	3.71
Average B				0.079	3.13
C	1	0.189	-3.70	0.135	4.54
C	2	0.558	-4.96	0.431	3.83
Average C				0.283	4.19
Overall Average		0.532	-4.91	0.424	3.06

13

Table II. Root mean square (RMS) errors of measured depths of fibrils*

(A) Vertically Oriented Fibrils

Reader	Image	RMS Error (mm)
A	1	0.59
A	2	0.62
B	1	1.91
B	2	1.78
C	1	1.53
C	2	0.75
Overall Average		1.20

(B) Horizontally Oriented Fibrils

Reader	Image	RMS Error (mm)
A	1	2.70
A	2	4.76
B	1	11.36
B	2	12.56
C	1	9.30
C	2	8.24
Overall Average		8.15

$$* \quad \text{RMS error} = \sqrt{\frac{\sum_{i=1}^{25}(\text{true depth}_i - \text{measured depth}_i)^2}{25}}$$

FIGURE CAPTIONS

FIGURE 1.   Diagram of the stereo phantom with simulated fibrils.   There are 6 layers of
1-mm-thick Lexan plates. In the design employed, one of the layers (the
second lowest one in this illustration) is superimposed with a 5 X 5 array of
fibrils randomly oriented in two directions. Each of the other five layers has 5
fibrils placed at randomly chosen locations, with the constraint that no more
than 2 fibrils will line up in the same location. The two fibrils at the same
location are always oriented perpendicular to each other. For clarity, only 5
fibrils in the top layer and 1 fibril in the bottom layer are drawn. The order of
the 6 layers was changed to create the two independent phantoms that were
analyzed by each viewer.

FIGURE 2.   **Top:**
Left and right eye images of the phantom shown in Fig. 1. The image pair
was obtained with a stereoscopic angle of $\pm 2.5^o$ about the central axis. The
fibril pairs with the smallest spacing of 2 mm in this phantom can be
identified and the relative depths of the different fibrils can also be clearly
distinguished.

Bottom:
Left: Image of the phantom that is stored in the computer frame buffer. This
image is synch-doubled by the display processor for stereoscopic viewing.
Synch-doubling enables viewing of the left- and right-eye images at twice the
nominal refresh rate of the display monitor for reduced flicker. The left-eye
image is stored in the frame buffer at the top, and the right eye-image at the
bottom. An additional vertical synch pulse is inserted between the two images
to produce the two separate images shown at the top of this figure.

Right: Image formed by combining the left and right images into one. An
image similar to this is seen when one views the display without the
stereoscopic glasses, and is the one used to calibrate the virtual cursor. The
virtual cursor (not shown above) appears as two cursors (a left eye cursor and
a right eye cursor) when the images are viewed without the stereo glasses, and
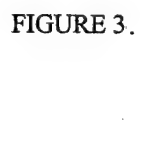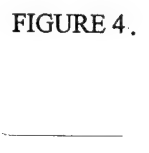the horizontal separation between the cursors changes as the cursor depth is
adjusted.

FIGURE 3.   Plots of the best and worst measured vs. true depths of the vertical fibrils for
the 3 readers. The plot with the best accuracy (r=0.994, SEE=0.38 mm) is
shown at the left, and the plot with the worst accuracy (r=0.887, SEE=1.33
mm) is shown at the right

FIGURE 4.   Plots of the best and worst measured vs. true depths of the horizontal fibrils
for the 3 readers. The plot with the best accuracy (r=0.947, SEE=1.24 mm) is
shown at the left, and the plot with the worst accuracy (r=0.135, SEE=4.54
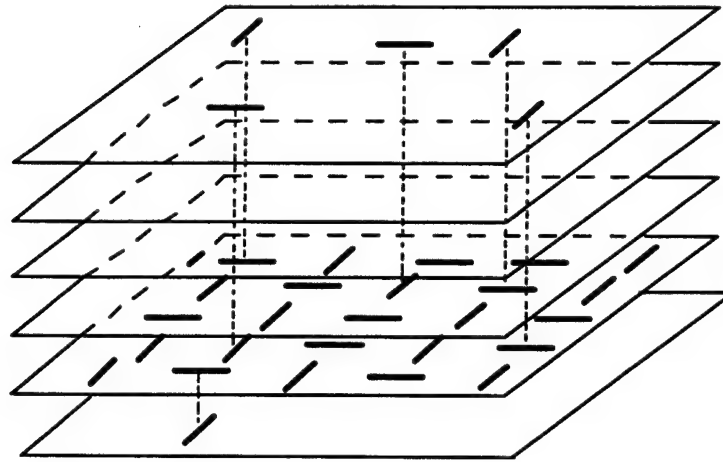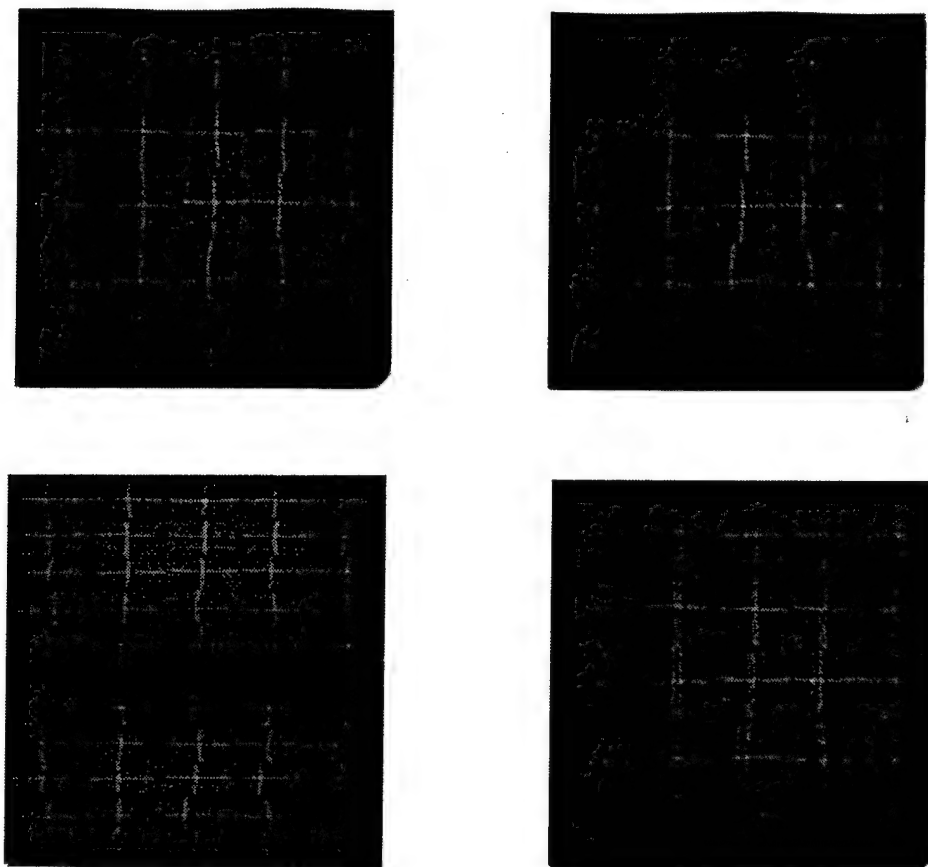mm) is shown at the right.

15

FIGURE 1.   Diagram of the stereo phantom with simulated fibrils.   There are 6 layers of
1-mm-thick Lexan plates. In the design employed, one of the layers (the
second lowest one in this illustration) is superimposed with a 5 X 5 array of
fibrils randomly oriented in two directions. Each of the other five layers has 5
fibrils placed at randomly chosen locations, with the constraint that no more
than 2 fibrils will line up in the same location. The two fibrils at the same
location are always oriented perpendicular to each other. For clarity, only 5
fibrils in the top layer and 1 fibril in the bottom layer are drawn. The order of
the 6 layers was changed to create the two independent phantoms that were
analyzed by each viewer.

FIGURE 2. **Top:**

Left and right eye images of the phantom shown in Fig. 1. The image pair was obtained with a stereoscopic angle of $\pm 2.5^o$ about the central axis. The fibril pairs with the smallest spacing of 2 mm in this phantom can be identified and the relative depths of the different fibrils can also be clearly distinguished.

Bottom:

Left: Image of the phantom that is stored in the computer frame buffer. This image is synch-doubled by the display processor for stereoscopic viewing. Synch-doubling enables viewing of the left- and right-eye images at twice the nominal refresh rate of the display monitor for reduced flicker. The left-eye image is stored in the frame buffer at the top, and the right eye-image at the bottom. An additional vertical synch pulse is inserted between the two images to produce the two separate images shown at the top of this figure.

Right: Image formed by combining the left and right images into one. An image similar to this is seen when one views the display without the stereoscopic glasses, and is the one used to calibrate the virtual cursor. The virtual cursor (not shown above) appears as two cursors (a left eye cursor and a right eye cursor) when the images are viewed without the stereo glasses, and the horizontal separation between the cursors changes as the cursor depth is adjusted.
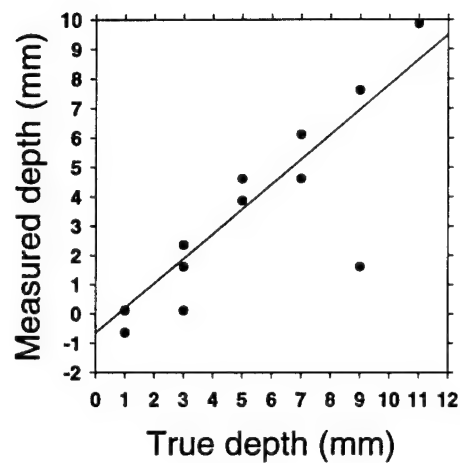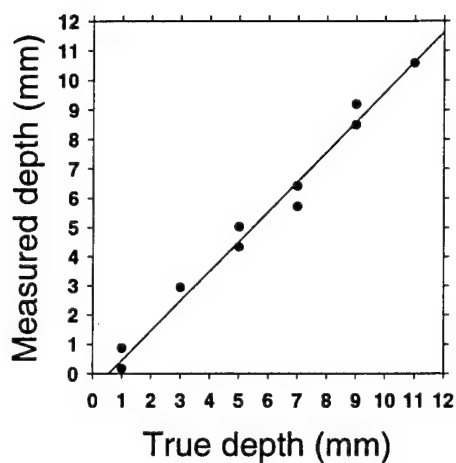
17

FIGURE 3. Plots of the best and worst measured vs. true depths of the vertical fibrils for the 3 readers. The plot with the best accuracy (r=0.994, SEE=0.38 mm) is shown at the left, and the plot with the worst accuracy (r=0.887, SEE=1.33 mm) is shown at the right.
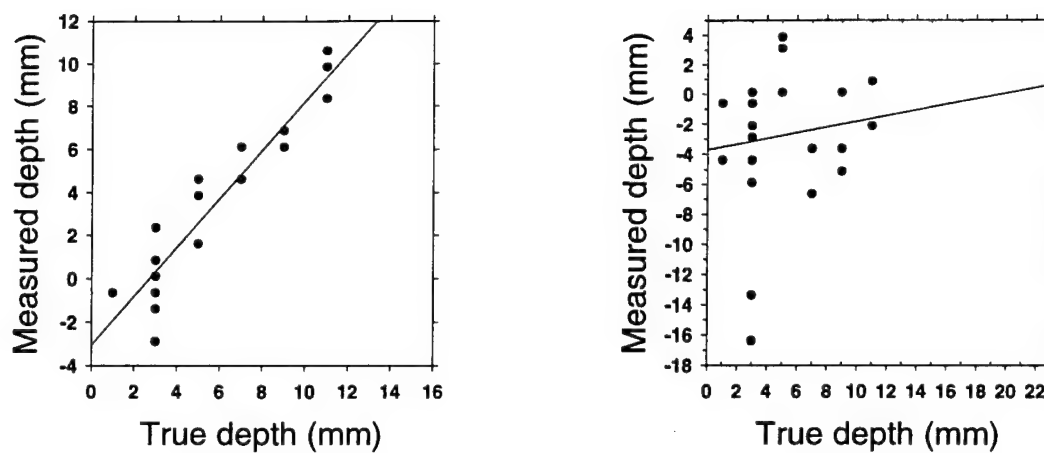
FIGURE 4. Plots of the best and worst measured vs. true depths of the horizontal fibrils for the 3 readers. The plot with the best accuracy (r=0.947, SEE=1.24 mm) is shown at the left, and the plot with the worst accuracy (r=0.135, SEE=4.54 mm) is shown at the right.

Effects of Stereoscopic Imaging Technique on Depth Discrimination

Heang-Ping Chan, Mitchell M. Goodsitt, Katie L. Darner, Jeffrey M. Sullivan,

Lubomir M. Hadjiiski, Nicholas Petrick, Berkman Sahiner

Department of Radiology, University of Michigan, Ann Arbor, MI 48109

Abstract

Stereoscopic mammography can potentially improve detection of breast cancer by reducing the effects of overlapping tissues and providing 3-dimensional information about a lesion. In this study, we evaluated the effects of imaging parameters on depth discrimination of mammographic features. A breast biopsy unit was used for digital image acquisition. A modular phantom containing 25 pairs of crossing vertical and horizontal fibrils with five different depth separations was designed. The phantom was sandwiched in the middle of 4 cm BR-12 material to simulate the scatter condition for an average breast. Stereoscopic image pairs of three different phantom configurations were acquired at $\pm 2.5^{\circ}$ and $\pm 5^{\circ}$ stereo-angles and at three different exposure levels. The images were displayed on a monitor and viewed with LCD stereo glasses. Nine observers visually judged if the vertical fibril in each pair of crossing fibrils was in front of or behind the horizontal fibril. It was found that for viewing fibrils, which simulated spiculations or thin fibrous structures in mammographic images, the accuracy of depth discrimination increased with increasing exposure and stereo-angle in the range studied. However, many observers found it difficult to merge the left-eye and right-eye images to achieve stereovision when the images were acquired with a large stereo-angle.

1

1.   Introduction

X-ray mammography is the most sensitive diagnostic method for detecting early breast cancers. However, a mammogram is a two-dimensional projection of a three-dimensional (3D) object. The anatomical structures along the x-ray beam path are projected onto an image plane and overlap with each other, resulting in one of the major limitations in mammography - low sensitivity for detecting lesions overlapping with dense fibroglandular tissues (Jackson *et al*, 1993). It was estimated that about 20% of the breast cancers in dense breasts are not detected by mammography (Wallis *et al*, 1991; Bird *et al*, 1992). The camouflaging effect of the overlapping structures is the main cause of missed diagnoses. Stereoscopic imaging may allow overlying structures to be perceived at different depths, thereby reducing the camouflaging effect.

Stereoscopic imaging requires acquisition of two images. The x-ray focal spot is shifted, along a direction parallel to the image plane, to the left and the right of the central axis to obtain two images of the object. The object and the detector have to remain stationary during the process. The images are referred to as the left-eye and the right-eye images. When the two images are placed properly and viewed by trained eyes or with the aid of a stereoscope so that the left eye sees only the left-eye image and the right eye sees only the right-eye image, the parallax between the two images creates the depth perception. Stereoscopic radiography has been attempted for different types of examinations (Doi *et al*, 1981; Kelsey *et al*, 1982; Doi and Duda, 1983; Higashida *et al*, 1988; Trocme *et al*, 1990; Ragnarsson and Karrholm, 1992). Stereoscopic imaging has not achieved widespread acceptance in clinical practice, however, mainly because of the doubled film cost and increased patient exposure (Curry *et al*, 1992). A secondary problem

is the need to train the eyes to perceive the stereoscopic effect without aid, or to use a special stereoscope, with careful arrangement of the films. The recent advent of direct digital detectors may make the stereoscopic technique a viable approach because no additional film cost will be required. Furthermore, a digital detector has a wider linear-response range and a higher contrast sensitivity than a screen-film system so that good-quality images may be acquired at a reduced radiation dose. Images in digital form can be subjected to image processing, further enhancing the visibility of the image details. Digital stereoscopic images can be viewed on a single display device with the assistance of stereoscopic goggles providing an electronic shutter. The stereoscopic images can therefore be displayed singly in the conventional manner or stereoscopically on the same viewing station to provide complementary diagnostic information.

One of the advantages of stereoscopic imaging is the 3D information it provides on the lesions of interest. It has been reported that the 3D distribution of microcalcifications may be correlated with the malignant or benign nature of the cluster (Conant *et al*, 1996; Maidment *et al*, 1996). Spiculations from a mass may also be more readily distinguished from overlapping tissues under stereoscopic viewing conditions. The additional diagnostic information may improve the classification of malignant and benign lesions, thereby reducing unnecessary biopsies and increasing the positive predictive value of mammography.

The usefulness of stereomammography depends on the depth perception of subtle mammographic features. The amount of stereoscopic shift has to match the imaging geometry in order to achieve the best depth perception. The signal-to-noise ratio of mammographic features

is determined mainly by the x-ray imaging techniques used. In this study, we evaluated the effects of imaging parameters on depth discrimination in stereomammographic imaging.

2. Materials and Methods

2.1 Phantom Design

We have designed a modular stereo phantom for this study. The phantom contains six 1-mm-thick Lexan sheets, each separated by 1-mm-thick spacers. Each Lexan plate contains a 5 X 5 array of object areas. Fifty nylon fibrils, each about 8 mm in length and 0.53 mm in diameter, are arranged in these object areas. Twenty-five fibrils are oriented vertically (perpendicular) and 25 horizontally (parallel) to the stereo shift direction. The fibrils are placed in the object areas on the six Lexan plates such that, in the projection image, each object area contains the projection of one vertical and one horizontal fibril that cross each other. The depth separation of each pair of crossing fibrils depends on the arrangement of the plates. These plates can be randomly ordered to produce many independent object configurations. In this study, the phantom with a 1-mm-thick cover plate (total thickness of Lexan in phantom = 7 mm) was sandwiched in the middle of 4-cm-thick BR-12 breast-tissue-equivalent material to simulate the scatter condition for an average breast.

2.2 Image Acquisition and Display

Digital stereoscopic image pairs were acquired with a Fischer Mammotest stereotaxic prone biopsy table. The system acquires digital images of 1024 X 1024 pixels and 12 bit gray levels in a 5 cm X 5 cm field of view using a fiber-optics-coupled CCD detector. No antiscatter grid is used with the digital detector. For this system, the automatic exposure technique at 26 kVp for a

4.2-cm-thick Lucite phantom is about 160 mAs. We acquired stereoscopic pairs of images at ±2.5° and ±5° stereo-angles using 26 kVp and 40, 70, 140 mAs per image. Three different configurations of the fibril phantoms were imaged under each exposure condition, producing 75 pairs of fibril images at 5 different depth separations under each condition. A training image was also acquired at 26 kVp and 10 mAs without the 4 cm BR-12 phantom.

Figure 1.   Stereoscopic display workstation.

The images were displayed on a 21" Barco-Metheus (Beaverton, OR) display monitor driven by a model 1760S stereoscopic board and a SUN Microsystems (Palo Alto, CA) Ultra 10 computer. The Metheus board displays 1408 x 1408 x 8 bit images at a refresh rate of 114 Hz. It operates in a page flipping stereoscopic mode with the left- and right-eye images displayed alternately.

NuVision (Beaverton, OR) LCD stereoscopic glasses were used for viewing the stereoscopic images. Figure 1 shows the stereoscopic display workstation used in this study.
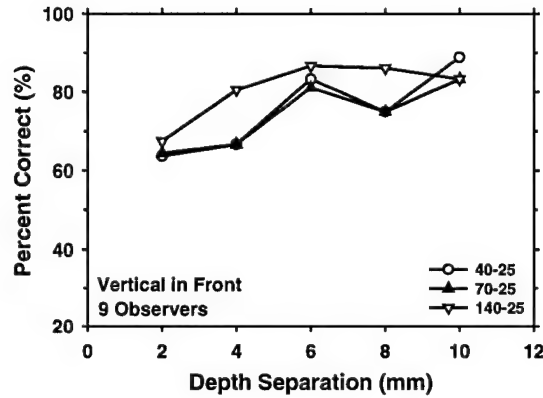
2.3 Observer Experiment

Nine observers participated in the experiment. A total of 18 stereoscopic image pairs (2 stereo-angles X 3 exposure levels X 3 phantom configurations) were viewed by each observer. Each image contained 25 crossing pairs of fibrils separated by one of five different spacings (2, 4, 6, 8, 10 mm). The observer was asked to visually judge if the vertical fibril in each pair of overlapping fibrils was in front of or behind the horizontal fibril. Each observer read the 18 images sequentially in a different pre-assigned randomized order. The reading orders of the observers were chosen so that, on average, no image acquired under a specific condition would be read more frequently in a certain order. This minimized the effects of observer learning, memorization, or fatigue on the reading results. The observer was not informed of the conditions under which the image being viewed was acquired. The training image was read before the experiment by each observer to familiarize him or her with the reading task.
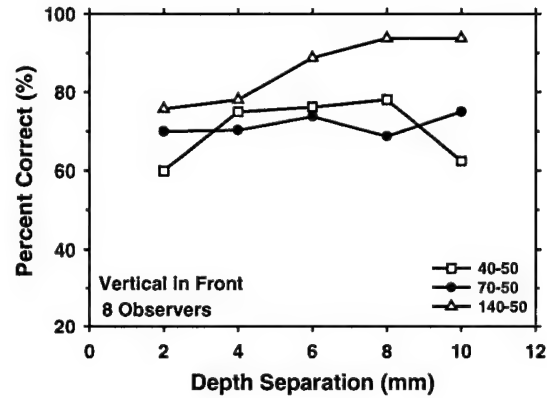
3. Results

It was found that the stereovision of the observers differed by a wide range and it appeared to depend on the quality of the stereoscopic images. All observers could perceive the stereoscopic training image with reasonable accuracy in judging the relative depths of the crossing fibrils. The fibrils in the training image had a higher contrast and signal-to-noise ratio than the test images. It was acquired without the 4 cm BR-12 phantom so that the scattered radiation was much lower than that in the test images. Some observers found it much more difficult to merge
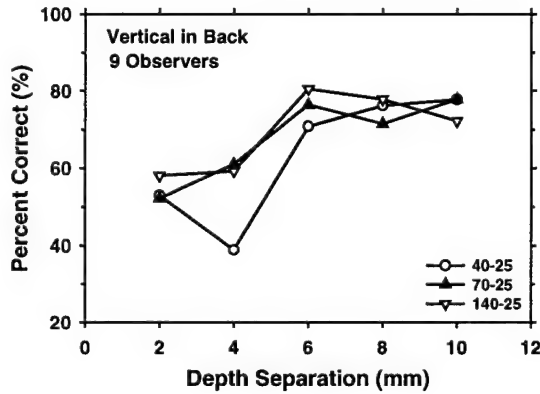
the left-eye and right-eye images to achieve a stereoscopic effect when they viewed the test images. This occurred more often with the images acquired at $\pm 5^{\circ}$ stereo-angle than those acquired at $\pm 2.5^{\circ}$ stereo-angle. One of the observers failed to merge the images at the $\pm 5^{\circ}$ stereo-angle so that the results at this angle were analyzed for only 8 observers.
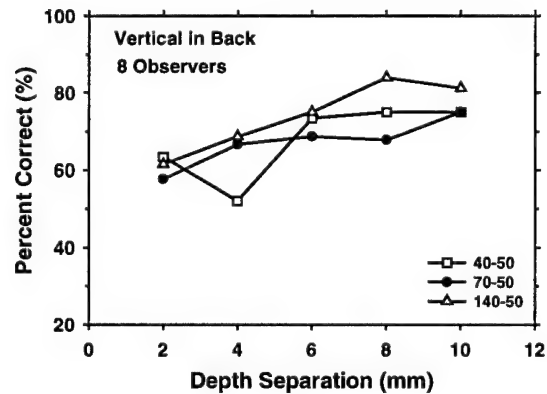

Figure 2.   Dependence of percentage of correct decisions, averaged over 9 ($\pm 2.5^{\circ}$) or 8 ($\pm 5^{\circ}$) observers, on depth separation and imaging conditions: (a) vertical fibril in front, $\pm 2.5^{\circ}$ stereo-angle, (b) vertical fibril in front, $\pm 5^{\circ}$ stereo-angle, (c) vertical fibril in back, $\pm 2.5^{\circ}$ stereo-angle, and (d) vertical fibril in back, $\pm 5^{\circ}$ stereo-angle. 40 mAs, 70 mAs, 140 mAs were used for image acquisition.

Figures 2(a)-(d) show the percentages of correct decisions plotted as a function of the depth separation of the crossing fibrils, averaged over 9 ($\pm 2.5^{\circ}$) or 8 ($\pm 5^{\circ}$) observers, for the different

imaging conditions studied. Because of the large variation in the accuracy of the observers, the standard deviations of the mean were large, ranging from 4% to 13%. The differences in the percentages of correct decisions between the different conditions were therefore not statistically significant. However, some trends can be observed. The curve for the highest exposure, 140 mAs, tended to be slightly higher than those for the other two exposures, except for a few points. The 140 mAs curves were also smoother than the other curves, indicating less variability in the readings. At this exposure level, the percentages of correct decisions appeared to increase by about 15 to 20% as the depth separation increased from 2 mm to 10 mm, and increase by an average of about 5% as the stereo-angle increased from $\pm 2.5^{o}$ to $\pm 5^{o}$, when other conditions were fixed. The percentages of correct decisions were 10 to 15% higher when the vertical fibrils were in front of the horizontal fibrils than when they were in the back.

Three of the observers had a higher accuracy in depth discrimination than the others. On average, their percentages of correct decisions were about 10% to 20% higher than the other 6 observers under most conditions, and were 40% to 50% higher in some cases. For these observers, it is more obvious that the accuracy was higher when the vertical fibrils were in front of the horizontal fibrils. For the smallest fibril separation of 2 mm, the accuracy was about 20% higher when the vertical fibril was in the front.

4.   Conclusion

This study shows that depth discrimination in stereomammography depends on imaging conditions and object configurations. For viewing of fibrils that simulated spiculations or thin fibrous structures in mammographic images, the accuracy of depth discrimination appeared to

increase with increasing exposure and stereo-angle. However, many observers found it difficult to merge the left-eye and right-eye images acquired with a large stereo-shift to achieve stereovision. Further studies will be conducted to evaluate the depth perception of different mammographic test objects. Studies are also underway to evaluate if specially designed cursors can assist in depth discrimination and measurement of absolute depths of target objects in stereoscopic images (Goodsitt *et al*, 2000a; Goodsitt *et al*, 2000b).

Acknowledgments

References

Bird, R. E., T. W. Wallace, and B. C. Yankaskas. 1992. Analysis of cancers missed at screening mammography. *Radiology* **184:** 613-617.

Conant, E. F., A. D. Maidment, M. Albert, C. W. Piccoli, S. A. Nussbaum, and P. A. McCue. 1996. Small field-of-view digital imaging of breast calcifications: method to improve diagnostic specificity. *Radiology* **201(P):** 369.

Curry, T. S., J. E. Dowdey, and R. C. Murry. 1992.*Christensen's Physics of Diagnostic Radiology.* (Fourth ed.) (Philadelphia, PA: Lea & Febiger).

Doi, K. and E. E. Duda. 1983. Detectability of depth information by use of magnification stereoscopic technique in cerebral angiography. *Radiology* **146:** 91-95.

Doi, K., N. J. Patronas, E. E. Duda, E. Geldner, and K. Dietz. 1981. X-ray imaging of blood vessels to the brain by use of mahnification stereoscopic technique. *Advance in Neurology* **30:** 175-189.

Goodsitt, M. M., H. P. Chan, and L. M. Hadjiiski. 2000a. Stereomammography: Evaluation of depth perception using a virtual 3D cursor. *Med. Phys.* (in press).

Goodsitt, M. M., H. P. Chan, J. M. Sullivan, K. L. Darner, and L. M. Hadjiiski. 2000b. Evaluation of the effect of virtual cursor shape on depth measurements in digital stereomammograms. The 5th International Workshop on Digital Mammography, Proc. IWDM: (in press). Toronto, Canada, June 11-14, 2000. (Madison, WI: Medical Physics Publishing).

Higashida, Y., Y. Hirata, R. Saito, S. Doudanuki, H. Bussaka, and M. Takahashi. 1988. Depth determination on stereoscopic digital subtraction angiograms. *Radiology* **168:** 560-562.

Jackson, V. P., R. E. Hendrick, S. A. Feig, and D. B. Kopans. 1993. Imaging of the radiographically dense breast. *Radiology* **188:** 297-301.

Kelsey, C. A., R. D. Moseley, S. A. mettler, and D. E. Briscoe. 1982. Cost-effectiveness of stereoscopic radiographs in detection of lung nodules. *Radiology* **142:** 611-613.

Maidment, A. D. A., M. Albert, E. F. Conant, C. W. Piccoli, and P. A. McCue. 1996. Prototype workstation for 3-D diagnosis of breast calcifications. *Radiology* **201(P):** 556.

Ragnarsson, J. I. and J. Karrholm. 1992. Factors influencing postoperative movement in displaced femoral neck fractures: evaluation by conventional radiography and stereoradiography. *J. Orthop Trauma* **6:** 152-158.

Trocme, M. C., A. H. Sather, and K. N. An. 1990. A biplanar cephalometric stereoradiography technique. *Am. J. Orthodontics and Dentofacial Orthopedics* **98:** 168-175.

Wallis, M. G., M. T. Walsh, and J. R. Lee. 1991. A review of false negative mammography in a symptomatic population. *Clinical Radiology* **44:** 13-15.

Evaluation of the Effect of Virtual Cursor Shape on Depth Measurements in Digital Stereomammograms

Mitchell M. Goodsitt, Ph.D., Heang-Ping Chan, Ph.D., Jeffrey M. Sullivan,

Katie L. Darner, and Lubomir M. Hadjiiski, Ph.D.

Department of Radiology

University of Michigan

Ann Arbor, MI

Table of Contents:

Introduction

The superposition of tissues is a major problem in conventional mammograms. It can result in the camouflaging of masses within dense tissues. It can also lead to false positive mass detection wherein objects that appear mass-like are formed by superimposed structures. The superposition problem can be reduced or eliminated by generating and viewing 3-D mammograms via techniques such as stereomamography. Stereomammography was first described in 1930 (Warren 1930). It involved taking two separate mammograms one at an x-ray tube angle of about $+3^\circ$ relative to the central axis, and the other at an angle of about -3°. These films were then viewed using special devices that employed mirrors or prisms to send one image to the observer's left eye and the other to the observer's right eye. Because this methodology required taking two films in roughly the same projection, it had several disadvantages including increased x-ray dose, expense, processing time, technologist time and radiologist viewing time. These disadvantages of film stereomammography eventually outweighed the 3-D visualization advantage, and film stereomammography was discontinued. Today's digital mammography machines eliminate or reduce most of the disadvantages, thereby making digital stereomammography a potentially viable technique. In particular, the linear response of the digital detectors makes it possible to utilize half the normal dose for each image. The observer's eye-brain system integrates the two images of the stereo pair to yield about the same signal-to-noise ratio as in a single image taken with the same total dose. Image processing and display are almost instantaneous, and viewing the images on a television monitor with LCD glasses that are synchronized so the left eye sees one image and the right the other is convenient and less time consuming than the film counterpart.

2

We have been employing a small field-of-view digital mammography system to investigate a new technique that is made possible through the integration of computer graphics with the stereoscopic image display. We generate a virtual 3-D cursor that can be calibrated to measure the depths of objects in digital stereomammograms. In our first studies, we investigated the accuracies of observers' measurements of the depths of horizontally and vertically oriented nylon filaments that simulated fibrils in mammograms (Goodsitt et al. 2000). We found that with a cross-shaped cursor, observers could measure depths of vertically oriented fibrils to 1-2 mm, but their accuracies were degraded for horizontally oriented fibrils. The purpose of the present study was to investigate whether the depth accuracy of the horizontally oriented fibrils might be improved through the use of a specially designed cursor.

Materials and Methods

We employed the images that were generated for our previous study (Goodsitt et al. 2000). These images were obtained with a Fischer (Denver, CO) MammoVision Stereotaxic unit using a stereo x-ray tube shift angle of $-2.5°$ to $+2.5°$. The phantom that was imaged consisted of six 1-mm thick Lexan sheets each separated by 1-mm spacers. A matrix of 8-mm long, 0.53 mm diameter nylon fibrils was placed on the plates with 25 fibrils oriented vertically (perpendicular) and 25 horizontally (parallel) to the stereo shift direction. The depths and orientations of the fibrils were randomized and organized such that one horizontal fibril crossed one vertical fibril at each of the 25 matrix positions. The order of the Lexan layers could be changed to create many independent phantom configurations. A photograph of the phantom appears in figure 1, below.
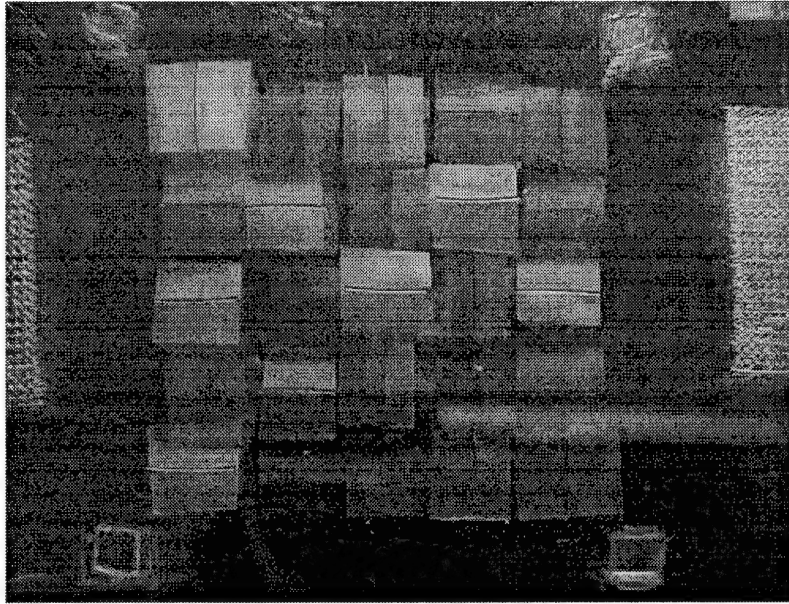
Figure 1: Front-view photograph of the phantom that was imaged

A commercial stereoscopic display with a cross-shaped virtual cursor (Neotek, Inc, Pittsburgh, PA) was employed in our previous study. This display utilizes a synch-doubling method to achieve stereo imaging at twice the normal refresh rate of a display monitor thereby minimizing flicker. This is a relatively inexpensive method for displaying high quality stereoscopic images. Its primary disadvantage is that it involves the storage of the left eye image above the right eye image in the computer frame buffer, and in order to accomplish this with most frame buffers, the vertical resolution of both images must be reduced by about a factor of two (e.g. two 1024 x 1024 images must each be reduced to about 1024 x 380 to fit in a 1024 x 768 frame buffer). For the present study, we developed software to display images and generate cursors of user selected shapes on a high-end stereoscopic display/viewing system. A Barco-Metheus (Beaverton, OR) model 1760S stereoscopic board was employed in a SUN Microsystems (Palo Alto, CA) Ultra 10 computer. The Metheus board operates in a page flipping stereoscopic mode whereby the full left and right eye images are displayed sequentially, one after the other. This board is capable of

displaying 1408 x 1408 x 8 bit images at a refresh rate of 114 Hz. The images in our study were displayed on a 21" Barco monitor and viewed with NuVision (Beaverton, OR) LCD stereoscopic glasses.

Software was written to allow the user to design and display virtual (stereoscopic) cursors and to display the x, y, and z positions of those cursors. The 3-D nature of the cursor is achieved by introducing offsets in the horizontal positions of the representations of the cursor in the left and right-eye images. The z-coordinate is equal to the offset. When the offset is 0, the cursor is at the same x, y position in both images, and it appears stereoscopically to be at the depth of the monitor screen. As the horizontal offset between the cursor positions is increased in one direction (e.g. left), the cursor appears to move closer to the observer, and as the offset is increased in the opposite direction (e.g. right), the cursor appears to move toward or into the monitor. The z-coordinate was calibrated by imaging thin wires placed on the steps of a stepwedge with known step heights. The stepwedge was imaged with the Fischer MammoVision system using the same x-ray tube shift as for the images of the fibril phantoms. The wires that were employed for calibration were oriented perpendicular to the tube shift direction. The resulting stereoscopic images were viewed without the stereo glasses and the left and right eye cursor positions were adjusted to overlay the left and right eye images of the wires on the steps. The z-coordinates of the cursor were linearly fit to the known depths of the wires to obtain the calibration line.

For the observer experiment, we had each participant use the stereoscopic virtual cursor system to measure the depths of 25 horizontally oriented fibrils in each of two images (two different

5

phantom configurations) for a total of 50 depth measurements per person. Each participant made these measurements twice using different cursors. One cursor was cross-shaped and the other was comb-shaped. The cursors are sketched in figure 2, below.
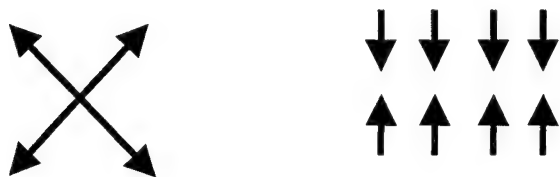

Figure 2: "Cross-shaped" and "fan-shaped" cursors employed in the experiment.

An artist's interpretation of the stereoscopic viewing apparatus appears in figure 3.
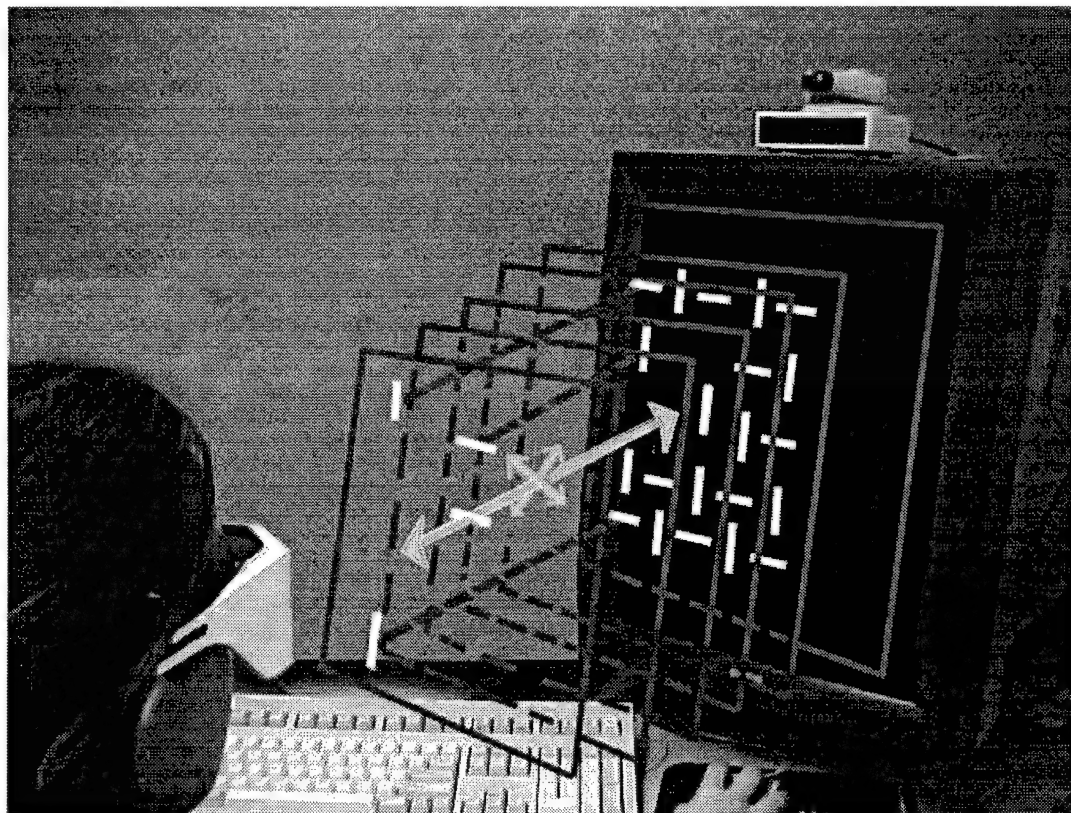

Figure 3: Graphical representation of the stereoscopic viewing system simulating the observer moving the virtual cursor within the stereo (3-D) image to match the horizontal fibril location.

The comb-shaped cursor was chosen because it provides the observer with more vertical depth cues. It was hoped that when the observer positioned the comb cursor such that the horizontal fibril appeared to move through the central slot as the cursor depth was varied, the additional depth cues might assist the observer in locating the depth of the fibril.

The observers recorded their measured z-coordinates of each horizontally oriented fibril, and these z-coordinates were converted to depths using the calibration line that was calculated from the stepwedge data discussed above. These depths were then compared with the known depths in terms of the parameters associated with least-square linear fits (slope, intercept, correlation coefficient (r-value), and standard error of the estimate (SEE)) of the measured depths to the true depths and in terms of the root mean square (RMS) errors of the measurements. The latter were computed using the equation:

$$\text{RMS error} = \sqrt{\frac{\sum_{i=1}^{50} (\text{true depth}_i - \text{measured depth}_i)^2}{50}}$$

Results

The results of the experiment are summarized in table 1, below.

Table1: Linear Fit Parameters and RMS Errors for Measured vs. True Depths

of Horizontally Oriented Fibrils

	Observer 1	Observer 1 Repeat	Observer 2	Observer 3	Observer 4
Slope (cross)	0.71	0.74	1.02	0.48	0.56
Slope (comb)	0.91	0.94	0.87	0.51	0.47
Intercept (cross)	0.44	1.09	-0.50	0.04	1.54
Intercept (comb)	0.79	0.63	0.75	1.94	1.11
r-value (cross)	0.80	0.83	0.94	0.55	0.48
r-value (comb)	0.98	0.97	0.95	0.60	0.49
SEE (cross) mm	1.70	1.58	1.20	2.32	3.28
SEE (comb) mm	0.64	0.72	0.95	2.16	2.68
RMS error (cross) mm	2.17	1.76	1.24	3.84	3.57
RMS error (comb) mm	0.76	0.80	0.98	2.68	3.50

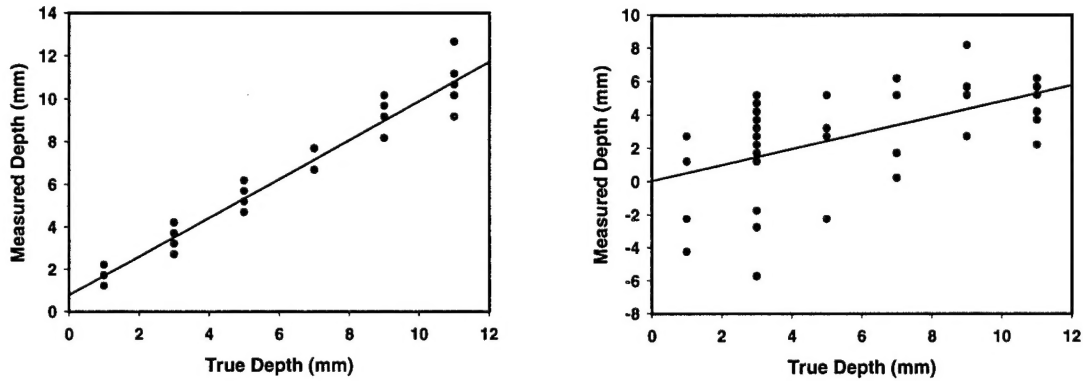Plots of the best and worst results are shown in figure 4, below.

Figure 4: Left: Best measured vs. true depth result (observer #1, comb cursor)

Right: Worst measured vs. true depth result (observer #3, cross cursor)

Discussion

Depth measurements made with the new comb-shaped cursor were more accurate. The RMS errors in the observers' measurements improved by 0.1 to 1.4 mm with this cursor relative to the cross-shaped cursor. In fact, with this new cursor, two of the observers were able to measure the depths of the horizontally oriented fibrils to an accuracy of about 1 mm, which approaches their accuracies for the vertically oriented fibrils in our previous study (Goodsitt et al. 2000). One of the observers repeated the entire experiment twice and those results appear in table 1 above. The linear fit parameters and RMS errors for the two trials by the same observer are very similar, indicating the results for that observer are very reproducible. The accuracies of all of the observers' measurements that are listed in table 1 do not tell the whole story. They do not reflect the amount of time required to make the measurements. In general, observers spent much more

time locating the positions of the horizontally oriented fibrils as compared with the vertically oriented fibrils. The observers would move the cursors in and out several times to hone in on the depths, which were much less obvious than the depths of the vertically oriented fibrils. The good results that were obtained indicate that the extra time and effort were worthwhile. Most objects in mammograms have orientations that are between horizontal and vertical, and even small vertical components make the depths easier to visualize and help reduce measurement times. We have designed an anthropomorphic breast phantom containing spiculated masses and microcalcification clusters at various known depths. In future studies, we will analyze the accuracies of depth measurements of the spiculations, microcalcifications and masses in that phantom with virtual cursors of different shapes and sizes.

Acknowledgments

References

Goodsitt M, HP Chan, LM Hadjiiski. 2000. Stereomammography: Evaluation of depth perception using a virtual 3D cursor. Accepted for publication, Med Phys.

Warren SL. 1930. Roentgenologic study of the breast. AJR 24:113-124.

DEPTH PERCEPTION IN DIGITAL STEREOSCOPIC MAMMOGRAPHY

Heang-Ping Chan, Mitchell M. Goodsitt, Jeffrey M. Sullivan, Katie L. Darner, and Lubomir M. Hadjiiski

University of Michigan Department of Radiology
Ann Arbor, MI 48109-0030

E-mail: chanhp@umich.edu

Stereoscopic mammography can potentially improve detection of breast cancer by reducing the effects of overlapping tissues and providing 3-dimensional information about a lesion. We developed display software for a high resolution, high refresh rate digital stereoscopic viewing system and created 3-D virtual cursors for measuring depths in stereo images. These tools were employed in observer experiments to evaluate the effects of imaging parameters on depth perception in stereomammography and to determine the effects of object orientation and virtual cursor shape on depth measurement accuracy.

A breast biopsy unit was used to produce digital stereo images of phantoms containing objects that simulated low-contrast fibrils in mammograms. For the imaging parameter experiments, images were acquired using +/- 2.5 and +/- 5 degree stereo-angles and 40, 70 and 140 mAs (dose) levels. The task was to judge whether a given fibril in a pair of overlapping horizontally and vertically oriented fibrils was in front of the other. For the virtual cursor experiments, depths were measured for fibrils that were oriented at 0, 45, 90, and 135 degrees. Both conventional cross-shaped and specially shaped cursors were employed.

We found that the error in depth discrimination increased with decreasing mAs and decreasing stereo-angle. The error was much lower and more consistent among observers when the vertical (90°) fibril was in the front. Studies using the cross-shaped virtual cursor showed that observers could measure depths of fibrils at 45, 90, and 135 degrees to within 1-2 mm. Depth measurements of horizontally oriented (0°) fibrils were far less accurate, but could be significantly improved using a cursor consisting of vertical lines with a horizontal slot through which the fibril would pass as the cursor depth was varied.

Depth discrimination in stereomammography depends on imaging conditions and object shapes and orientation. Virtual cursors can be employed in digital stereomammography to measure depths of fibril-simulating objects to about 1-2 mm. The shapes of the virtual cursors can be tailored to improve accuracy for specific depth measurement tasks.

METHOD AND MATERIALS: Images were made at several different radiographic techniques using equal doses on a Kodak Min-R 2000 system and on a prototype full-field digital unit that used a CsI phosphor and amorphous silicon detector. For each target/film/kVp combination (Mo/Mo/26, Mo/Rh/28, Rh/Rh/30), exposures at 10 different mAs settings were made. This resulted in images that had film optical densities ranging from 0.21 to 4.2. Three observers read each image and determined the number of disks visible for each contrast level. SNRs were measured directly from the images by calculating the difference between the mean pixel value inside and outside the disk; and, by calculating the standard deviation in the mean pixel value in ten different regions of equal size and shape to the disk, sampled outside the disk. In addition, the SNRs were calculated using the standard formula based on modulation transfer function, noise power spectrum, characteristic curve, and exposure data for each system.

RESULTS: Visually, the digital images were superior to the screen-film images in over 90% of the comparisons (i.e. more disks were visible in the digital images). This was particularly true for images taken at low and high mAs. The measured and calculated SNRs showed good agreement within experimental error. There was general agreement between the observer results and the calculated SNRs after incorporating the human visual system response into the calculation.

CONCLUSIONS: Full-field digital mammograms have higher image quality (i.e., higher SNR) than screen-film mammograms over a wide variety of exposure conditions. (RMN is a shareholder in R2 Technology, Inc. (Los Altos, CA).)

1165 · 2:39 PM

Comparison of Conventional Screen-Film Mammography and a Direct Digital Magnification System: Detection of Simulated Small Masses and Calcifications with Usual and Reduced Dose

K. Hermann, PhD, Goettingen, Germany · M. Funke, MD · E.H. Grabbe, MD

PURPOSE: Comparison of a direct digital magnification mammography system using a large-area amorphous silicon image receptor and a conventional screen-film mammography system with regard to the detection of simulated small masses and calcifications. Evaluation of the impact of a dose reduction with the digital flat-panel detector was of special interest.

METHOD AND MATERIALS: A scitillator coupled self-scanning flat-panel detector, based on amorphous silicon technology with 127 x 127 μm pixel size, 2,232 x 3,200 matrix and 16 bit digital output was used. This digital detector was part of a new magnification mammography system, which performs full-sized overview mammograms in 2.1fold magnification. The direct digital system was compared with a state-of-the-art conventional mammography system. Images were taken at the same dose as screen film mammograms and at significantly reduced doses. A contrast-detail mammography phantom (CDMAM) consisting of an aluminum base with gold disks of orderly decreasing thickness and diameter located in small sqares in a 16 x 16 matrix simulating both small masses and calcifications was used to estimate the contrast-detail resolution. The correct observation ratio (COR) as a figure of the detail resolution was calculated as the percentage of correctly identified disks of the total number of disks. Receiver operating characteristic (ROC) analysis was performed for observations made by three independent observers. Student's *t* test (95% confidence-level) was used for statistical analysis.

RESULTS: ROC analysis showed that images taken with the direct digital mammography system at the same dose as screen-film mammograms were significantly superior to this conventional images with respect to the detectability of small masses and calcifications. The digital system with almost bisected dose achieved the COR values of conventional screen-film mammography.

CONCLUSIONS: The results of this phantom study indicate that a amorphous silicon detector technology in combination with direct magnification technique holds promise in terms of dose reduction in mammography without loss of diagnostic accuracy compared with conventional screen-film mammography.

1166 · 2:48 PM

A Dual-Energy Subtraction Imaging Technique for Enhanced Mircrocalcification Imaging and Tissue Composition Measurement in Digital Mammography

(FDA)

C.C. Shaw, PhD, Houston, TX · X. Liu, PhD · G.J. Whitman, MD

PURPOSE: To describe and demonstrate a dual-energy subtraction imaging technique to enhance microcalcification imaging and to obtain tissue composition measurements.

METHOD AND MATERIALS: A dual-energy subtraction technique was used to generate two images representing the adipose and glandular tissue thickness on a pixel-by-pixel basis, respectively. The total breast thickness information was added to separate and image a third attenuating material: calcification. The two thickness images were also used to generate a

pixel-by-pixel measurement of tissue composition. Theoretical and numerical studies were conducted to investigate the properties of the calcification signals and effects of various parameters including the x-ray kV_p/filtration, breast thickness and composition, exposure distribution and scatter-to-primary ratio. Phantom images were obtained with digital mammography units to demonstrate the feasibility of this technique.

RESULTS: It has been shown that the calcification signals are proportional to the thickness of the calcifications. The calcification signal-to-noise ratios are degraded. However, the structured background of tissue contrast was largely removed, resulting in improved visualization of microcalcifications. Although radiation scatter resulted in un-cancelled background, the residual background signals were small and smooth. Tissue composition measurements from the subtraction images were significantly affected by the presence of scatter. Its accuracy remains to be improved by scatter rejection or correction methods.

CONCLUSIONS: It is feasible to use dual-energy subtraction imaging technique to enhance the visualization of microcalcifications and to obtain tissue composition measurements. (This work was supported by a grant CA51248 from the National Cancer Institute and a grant from the Mike Hogg Foundation.)

1167 · 2:57 PM

Stereomammography: Evaluation of Depth Perception Using a Virtual 3D Cursor

M.M. Goodsitt, PhD, Ann Arbor, MI · H. Chan, PhD · L.M. Hadjiiski, PhD

PURPOSE: We are evaluating the usefulness of stereomammography in improving breast cancer diagnosis. One area we are investigating is whether the improved depth perception associated with stereomammography might be significantly enhanced with the use of a virtual 3-D cursor. A study was performed to evaluate the accuracy of absolute depth measurements made in stereomammograms with such a cursor.

METHOD AND MATERIALS: A biopsy unit was used to produce digital stereo images of a phantom containing 50 low contrast fibrils (0.5 mm diameter monofilaments) at depths ranging from 0 to 10 mm, with a minimum spacing of 2 mm. Half the fibrils were oriented perpendicular (vertical) and half parallel (horizontal) to the stereo shift direction. The depth and orientation of each fibril were randomized, and the horizontal and vertical fibrils crossed simulating overlapping structures in a breast image. Left and right eye images were generated at angles of +/- 2.5 degrees. Three observers viewed these images on a computer display with stereo glasses and adjusted the position of a cross-shaped virtual cursor to best match the perceived location of each fibril. The x, y and z positions of the cursor were indicated on the display. The z (depth) coordinate was separately calibrated using known positions of fibrils in the phantom. The observers analyzed images of two configurations of the phantom. Thus, each observer made 50 vertical filament depth measurements and 50 horizontal filament depth measurements. These measurements were compared with the true depths.

RESULTS: The correlation coefficients between the measured and true depths of the vertically oriented fibrils for the 3 observers were 0.99, 0.97, and 0.89 with standard errors of the estimates of 0.39 mm, 0.86 mm, and 1.39 mm. Corresponding values for the horizontally oriented fibrils were 0.91, 0.28, and 0.08, and 1.91 mm, 4.37 mm, and 3.33 mm.

CONCLUSIONS: All observers could estimate the absolute depths of vertically oriented objects fairly accurately in digital stereomammograms; however, only one observer was able to accurately estimate the depths of horizontally oriented objects. This may relate to different aptitudes for stereoscopic visualization. The orientations of most objects in actual mammograms are combinations of horizontal and vertical. Further studies will be performed to evaluate absolute depth measurements of fibrils oriented at various intermediate angles and of objects of different shapes. The effects of the shape and contrast of the virtual cursor on the accuracy of the depth measurements will also be investigated.

1168 · 3:06 PM

Comparison of Contrast-Detail Characteristics of Tomosynthetic Reconstruction Techniques for Digital Mammography

S. Suryanarayanan, MS, Worcester, MA · A. Karellas, PhD · S. Vedantham, MS · S.J. Glick, PhD · C.J. D'Orsi, MD · R.L. Webber, DDS, PhD

PURPOSE: To compare different tomosynthetic reconstruction techniques on the basis of their contrast-detail characteristics in a cluttered background.

METHOD AND MATERIALS: A contrast-detail phantom was fabricated with cluttered structures surrounding objects of interest, which were holes ranging from 0.18 mm to 4.82 mm in diameter and 0.06 mm to 0.73 mm in depth (Med-Optics, Tucson, AZ). A clinical prototype full-field flat panel mammographic imager (GE Medical Systems) was used throughout the study. The data were acquired at 7 discrete angles (in 60 steps)by moving the x-ray source through a 360 arc. The planar images were acquired at 26 kVp, 80 mAs and 26 kVp, 225 mAs respectively. The exposure parameters used for tomosynthesis were 26 kVp, 10 mAs/view and 26 kVp, 32